Scanning Microscopy

Volume 1990
Number 4 *Fundamental Electron and Ion Beam Interactions with Solids for Microscopy, Microanalysis, and Microlithography*

Article 19

1990

Ion-Induced Electron Emission from Solids

Wolfgang O. Hofer
KFA Jülich

Scanning Microscopy Supplement 4, 1990 (Pages 265-310) 0892-953X/90$3.00+.00
Scanning Microscopy International, Chicago (AMF O'Hare), IL 60666 USA

ION-INDUCED ELECTRON EMISSION FROM SOLIDS

Wolfgang O. Hofer*

Projekt Kernfusion, KFA Jülich, D-5170 Jülich, Germany
and
Solid State Division, Oak Ridge National Laboratory,
Oak Ridge, TN 37831, U.S.A.

Abstract

A review of ion-induced electron emission is presented which concentrates on the mechanisms relevant to imaging, analysis, and processing of surfaces by ion beams. In this field of applications, the main interest in electron emission lies in kinetic emission by heavy, i.e. multi-electron ($Z > 2$) ions of energy $\leq$ 100 keV.

KEY WORDS: Electron emission, solid, ions, electron distribution, electron energy

*Address for correspondence (and present address):
Projekt Kernfusion,
KFA Jülich,
D-5170 Jülich,
Germany
Telephone No.: (49) 2461-616368

Contents

List of Symbols

a_H	Bohr's radius of the H-atom
$\cos^{-1}\alpha \equiv 1/\cos\alpha$	
$dE/dx)_{elec}$	electronic stopping power of the target for the incident projectiles; only where necessary is the index "p" added to distinguish it from the stopping power for internal electrons
$dE/dx)^e_{elec}$	electronic stopping power of the target for internal electrons
$dE/dx)_{nucl}$	nuclear stopping power
ϑ_p	polar angle of projectile incidence
E	energy, mostly of emitted electrons
$\hat{E}$	most probable energy of emitted electrons
$E_{e,max}$	maximum energy transferred to an electron in an elastic collision
E_F	Fermi energy in free electron gas of metals
E_{io}	ionisation energy of an atom
E_{in}	kinetic energy of internal electrons
E_p	projectile energy
E_{sb}	surface barrier energy, mostly of electrons; only where a distinction between electrons and atoms is necessary are the respective indices added
ε	Lindhard's reduced energy
$F_{d,a}(x=0)$	energy deposited in the surface in the form of atomic motion
$F_{d,e}(x=0)$	energy deposited in the surface in the form of electronic excitation
Φ_w	work function
γ_{pot}	electron yield by potential emission
γ, $\bar{\gamma}$	(average) integral kinetic electron yield; integral here means integrated over the whole energy and emission-angle spectrum. Potential emission is not included.
$j(E,\Omega)$	flux density of electrons emitted with energy E in the direction Ω
λ_e	escape depth of electrons from solids
Λ_a	target-specific constant in SIGMUND's sputtering yield formula
Λ_e	target-specific constant in SCHOU's electron yield formula
M	atomic mass (index "p": of projectile, "t": of target); in amu
$N_{in}(x,E_{in},\Omega_{in})$	number density of internal electrons at depth x with energy E_{in} and momentum direction Ω_{in}
p	momentum of electrons (index "in": internal electrons)
$P(\gamma;\bar{\gamma})$	probability of the emission of γ electrons per individual projectile impact; here, γ is an integer number and $\bar{\gamma}$ the average yield; $P(\gamma;\bar{\gamma})$ is also referred to as the probability distribution of electron emission, or the electron emission statistics; a Poisson distribution is a good but not always satisfying approximation.
v_H	Bohr's velocity
v_p	projectile velocity
Y	sputtering yield
Z	atomic number (index "p": of projectile, "t": of target)

1. History and Outset

Electrical discharges in rarified gases were the experimental tool in atomic physics for the 75 years following FARADAY's studies in the 1830's. The discovery of x-rays, of the electron, of the plasma-state of matter, as well as the development of experimental techniques such as the generation of canal and cathode rays, mark the exploration of an immensely resourceful phenomenon. It thus appears absurd that the understanding of the very driving force of self-sustained gas discharges, namely the ion-impact-induced emission of electrons from the cathode and their subsequent ionizing collisions, came at a time when discharge phenomena had ceased to be of central interest. In fact, it was a technical spin-off, GOLDSTEIN's canal-ray technique, which allowed the identification of the "radiation of negative electricity" from the cathode as electron radiation, and the determination of the characteristics of this emission phenomenon, FÜCHTBAUER (1906a,b). In this and all further investigations, the gas discharge merely

served as a source of ions; the actual emission investigation was carried out in a separate chamber where the solid no longer served as cathode to the discharge, but was subject to the ion radiation only.

The answer to the question of who "discovered" ion-induced electron emission is a matter of interpretation of turn-of-the-century publications, VILLARD (1899), THOMSON (1904), FÜCHTBAUER (1906a,b); the problem lies in the uncertainty of the perception of the *electron* at the time the phenomenon became apparent. It is beyond doubt, however, that it was FÜCHTBAUER who performed the first experiments under reasonably defined conditions and thereby established most of the characteristic features of ion-induced electron emission. Since it appears that this pioneering work is disregarded in the more recent reviews, we shall use FÜCHTBAUER's statements as a guideline through this overview. Particular interest will be devoted to the mechanisms relevant to heavy ion bombardment in the 1 to 100 keV regime. This is the area of greatest importance in applications such as ion detection and the imaging of surfaces. It is also the area of greatest physical complexity, since there are several ejection mechanisms which compete and which have differing efficiencies with changing bombardment and target conditions. The term "heavy" ion is synonymous here with *multi-electron* ion or projectile. This covers all particles higher in atomic number than helium. The reason for this distinction at Z = 2 lies in the excitation mechanism and will become clear in the following chapter. The actual inertia of the projectile is of secondary importance in this field, where *electronic* interaction lies in the foreground of interest.

Put into present-day terminology, FÜCHTBAUER (1906a,b; 1907) stated:

- the **electron yield**, i. e. the number of emitted electrons per incident ion, increases with increasing energy and incidence angle of the ions (cf. Chap. 4.2 and 4.3); the yield depends, furthermore, on the solid's surface condition, and it correlates with the position of the solid in the electromotive series (Chapter 4.4); those metals which have the highest yields show also the lowest cathode drop (sheath potential) in gas discharges.
- the **angular distribution** is diffuse, as opposed to specular emission; the emission intensity decreases with increasing angle of emission with respect to the surface normal (Chap. 4.5).
- the **energy distribution** is strongly peaked at low energies, and is almost independent of the projectile's energy and angle of incidence; moreover, it

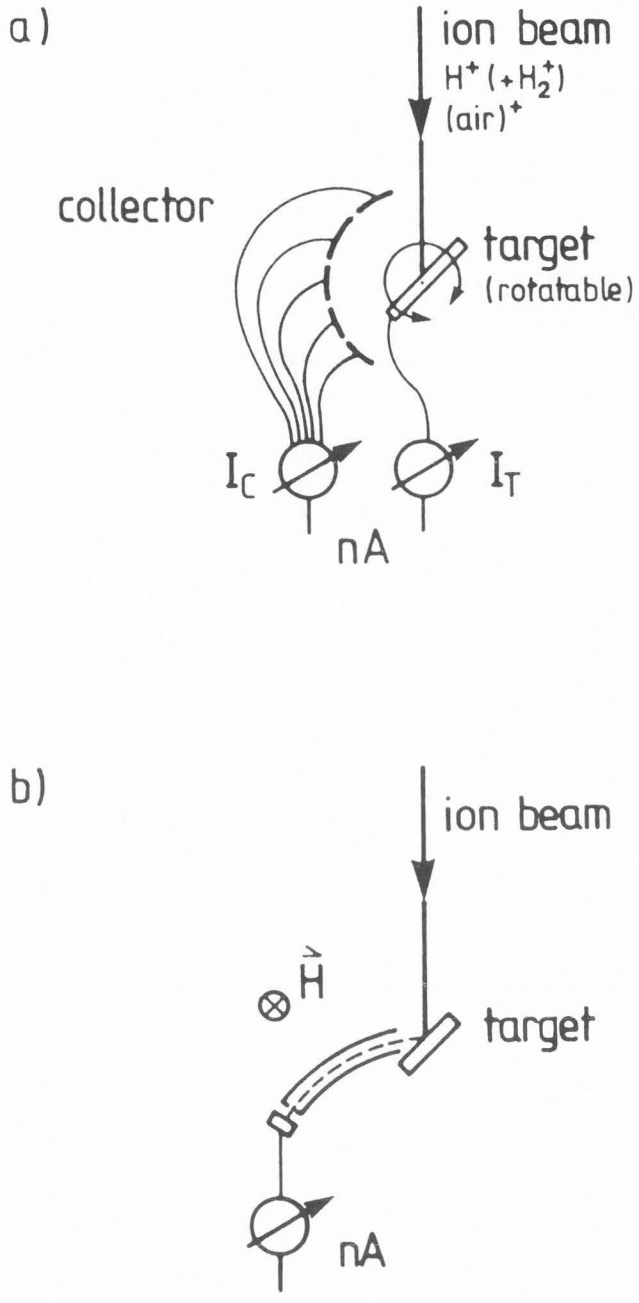

Fig. 1.1: FÜCHTBAUER's (1906a,b; 1907) experimental set-up for studying ion-induced electron emission. Hydrogen canal rays were used in most of his experiments.
a) Schematics of the set-up to measure integral and angular-resolved electron yields with a segmented collector.
b) Schematics of the set-up to measure the energy distribution of emitted electrons.

is identical to the energy distribution of secondary electrons[1], i.e. electrons emitted upon *electron* impact, (Chap. 4.6).

- the negative radiation from α-sources, THOMSON (1904), the induced negative radiation from solids exposed to α-particle radiation, RUTHERFORD (1905), and the electrons emitted from solids bombarded with canal-ray ions, FÜCHTBAUER (1906a,b), are all related effects.
- the energy of the electrons is determined by the target atoms, not by the energy of the incident projectile.

The experiments were performed by employing mostly hydrogen canal rays and the techniques sketched in Fig.1.1. It will be apparent in the following discussion that none of these statements is incorrect. Some of them are rather qualitative and speculative, but the overall picture developed was the key to the full understanding of the cathode rays and the cathode-drop phenomenon in self-sustained gas discharges. Moreover, until the work of BECKER (1924,1925) and OLIPHANT (1930) it was to be the only investigation which aimed at an understanding of the radiation-induced electron emission phenomenon as a whole, instead of dealing with details of emission characteristics.

2. The Mechanisms of Ion-Induced Electron Emission

It became clear with the work of HOLST and OOSTERHUIS (1921), and OLIPHANT (1930) that ions may release electrons from solids in two ways: by virtue of their kinetic energy in a collisional energy-transfer process, and by virtue of their potential energy, stored in the form of ionization energy. The total electron yield, therefore, consists of two components, the kinetic electron yield γ, and the potential electron yield γ_{pot},

$$\gamma_{tot} = \gamma + \gamma_{pot} \qquad (2.1)$$

2.1. Potential Emission

Potential emission of electrons is caused by radiationless neutralization and de-excitation of ions, or de-excitation of electronically excited neutrals approaching the surface of a solid. An electron from the solid tunnels to the empty state of the ion (excited neutral) whereby the released energy is transferred to another electron of the solid. This particular process - there exist modified forms with resonance transitions - is referred to as Auger-neutralization; it is sketched in Fig.2.1 for the case of an ion near a metal surface.

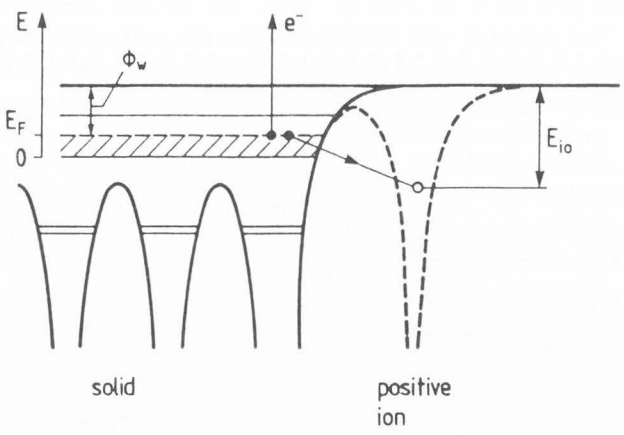

Fig. 2.1: Neutralization of an ion in the vicinity of a metal surface by a nonradiative transition, where the liberated energy of $E_{io} - \Phi_w$ is transferred to a conduction electron. The mechanism sketched here is referred to as Auger neutralization.

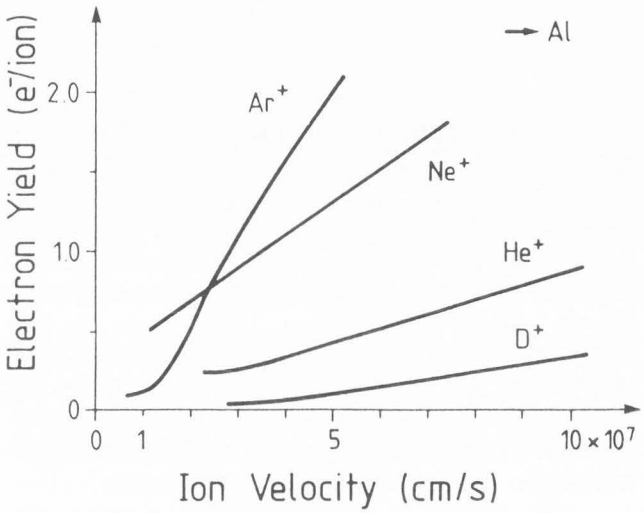

Fig. 2.2: Velocity dependence of the electron yield for various singly charged ions incident on Al. From ALONSO et al. (1980).

Since the maximum energy which can be transferred to an electron in the solid is $E_{io} - \Phi_w$, where E_{io} is the ionization energy and Φ_w is the work function, emission to the vacuum level requires

$$E_{io} - \Phi_w > \Phi_w \quad \text{or} \quad E_{io} > 2 \cdot \Phi_w \qquad (2.2)$$

For singly charged ions approaching the surface of normal metals ($\Phi_w \geq 3$ eV), potential

[1]Except for the reflected-electron peak. Electron-induced electron emission from solids was discovered only four years earlier by AUSTIN and STARKE (1902).

emission is significant only for He^+ (E_{io} = 24.5 eV) and Ne^+ (E_{io} = 21.6 eV). This is obvious also from an empirical relation suggested by BARAGIOLA et al. (1979a) according to which the electron yield is given by

$$\gamma_{pot} \approx 3 \times 10^{-2} \{ 0.8 \cdot E_{io} - 2\Phi_w \} \quad (2.3)$$

Under the conditions envisaged here ($E_{io} \leq 10$ eV, $\Phi_w \geq 3$ eV), the yields by potential emission are significantly smaller than unity, see, for example, the yields extrapolated to small velocities in Fig.2.2. Clearly, for singly charged ions at impact energies $E_p > 1$ keV the dominating emission process is *kinetic* emission. The picture changes though for multiply charged ions, see, for instance, the review by VARGA (1987) or the recent papers by LAKITS et al. (1989a,c), but multiply charged ions are beyond the scope of this overview.

In keeping with the topic of this conference, this overview addresses especially the electron-emission processes encountered in the imaging and analyzing of surfaces by ion bombardment. In this field, potential emission of electrons is of limited importance. For this reason, we restrict ourselves henceforth to kinetic emission. We should like to note here, however, that the *velocity dependence of potential electron emission* is only poorly known. Problems arise, therefore, when kinetic emission is to be separated from potential emission in cases where both components are of comparable magnitude. For singly charged ions this applies to ions of high ionization potential at velocities $v_i < 10^7$cm/s. An example of this situation is displayed in Fig.2.2 for He^+ and Ne^+. With multiply charged ions the problem becomes acute. It is presently a matter of intensive research, FEHRINGER et al. (1987), de ZWART (1987), DELAUNAY et al. (1988), LAKITS et al. (1989), ZEHNER et al. (1986).

2.2 Kinetic Emission

Contrary to potential emission, the excitation of electrons in kinetic emission is not confined to the surface but extends into the bulk along the projectile's track. Emitted electrons, on the other hand, stem from a rather shallow depth, the escape depth λ_e, as it is called (Fig.2.3). It is, therefore, natural to subdivide the phenomenon into three processes:

- **excitation** of electrons in the solid,
- **transport** of excited electrons towards the surface, and
- **emission** of electrons from the surface.

Only the excitation step is fundamentally different for heavy-ion, light-ion, and electron projectiles.

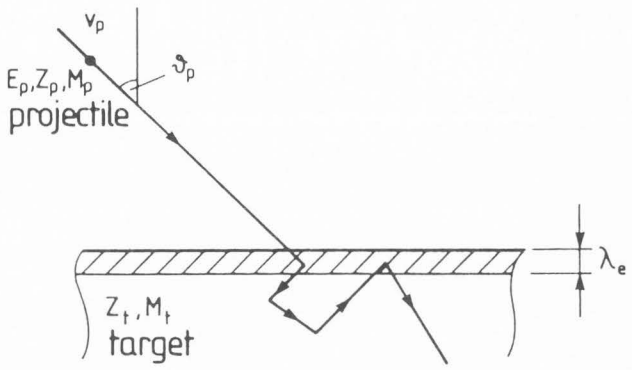

Fig. 2.3: Nomenclature for projectile-impact and target quantities. λ_e is the escape depth of electrons excited in the solid.

Transport of excited electrons and the emission proper are primarily determined by target properties and are, therefore, largely independent of the projectile species. For this reason, all the emission characteristics discussed in Chap.4 are primarily target-influenced, the only exception being the dependence of the yield on the projectile's electron shells (Chap.4.4).

2.2.1 Formal Correlations with the Collisional Emission of Atoms. Kinetic electron emission shows remarkable similarities to the collisional emission of atoms from surfaces, i.e. physical sputtering. These similarities pertain to the energy and angular distributions, the influence of the crystal lattice on the yields, the magnitude of the yields as well as their fundamental dependency on the projectile energy, and go finally as far as the development of successful theoretical concepts. Such far-reaching similarities between electron and atom emission may not be supposed from the outset since these two phenomena are effects of two different interaction regimes of energetic particles with matter:

In energetic particle/solids collisions, a distinction is made between nuclear and electronic interactions. This distinction is particularly clear and logical for metal targets, where the nuclear interaction is primarily responsible for the motion of the atoms - including the ensuing defect structure in the lattice -, and the electronic interaction to that of the electrons. Such a decoupling of the effects of electronic and nuclear collisions meets restrictions with insulators, where atomic motion is caused by electronic collisions as well.

In **nuclear collisions**, the kinetic energy of the collision partners is conserved. This applies to the

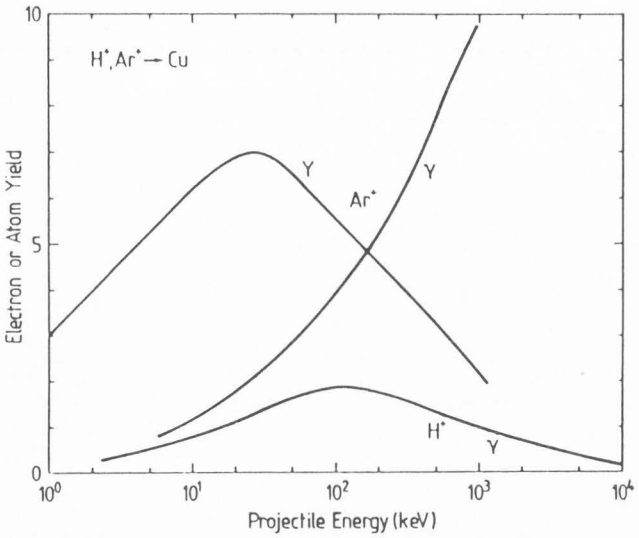

Fig. 2.4: Energy dependence of the electron yield from copper irradiated with H^+ and Ar^+ ions. For comparison, the sputtering yield for Ar^+ ions is also shown; this is a case where good correlation exists between the yield and nuclear stopping. A similarly satisfying correlation between electronic stopping and electron emission is found only for light-ion bombardment. For projectiles heavier than He^+, here Ar^+, there is no direct proportionality between γ and $dE/dx)_{elec}$. Unfortunately, no yield-data sets are available at and beyond the maximum for projectiles heavier than hydrogen.

collisions between the projectile and target atoms, as well as to collisions between recoiling target atoms. The average energy loss of the projectile per unit path length due to nuclear collisions is referred to as the *nuclear stopping power*, $dE/dx)_{nucl}$ of the target with respect to the given projectile. The slowing-down process due to nuclear collisions is a distribution of kinetic energy from one energetic particle to an ever increasing number of target atoms. Eventually a *cascade* of recoils is formed. The treatment of the development of nuclear collision cascades in space and time is a domain of transport theory. Where the collision cascade intersects the surface, atoms are ejected. Ejection requires a certain minimum amount of kinetic energy of the recoiling atoms in order to allow them to overcome the surface binding energy, $E_{sb,a}$. As a first approximation, the sublimation energy is usually taken as the surface barrier height. For metals, this barrier height is thus of the order of $E_{sb,a} = 5 \pm 3$ eV.

In the theory of sputtering developed by SIGMUND, the yield Y is proportional to the amount of energy deposited in the form of atomic motion in the surface, $F_{d,a}(x=0)$,

$$Y = \Lambda_a \cdot F_{d,a}(x=0) \qquad (2.4)$$

where Λ_a is a material constant which is inversely proportional to the surface binding energy $E_{sb,a}$. $F_{d,a}(x=0)$ is, in its essence, given by the nuclear stopping power of the target at the entrance of the projectile. Hence,

$$Y \propto E_{sb,a}^{-1} \cdot dE/dx)_{nucl}. \qquad (2.5)$$

An illustrating example of this proportionality is shown in Fig.2.4 for the case of the *sputtering* yield of Cu by Ar^+ bombardment. The corresponding case for electronic interaction, namely that of the electron-yield dependence upon H^+ bombardment, is also shown for comparison.

The interaction regime complementary to nuclear collisions is that of **electronic collisions**. Here, the energetic projectile interacts with the bound electrons of the target's ion cores and, where present, with free electrons. The energy loss per unit path length effected by the target in these collisions is referred to as the electronic stopping power, $dE/dx)_{elec}$. A fraction of this energy transferred to electrons is given to them in the form of kinetic energy, and these excited electrons will collide with other electrons. Again a cascade develops, an electron cascade which can be treated by Boltzmann equations. And again, from that fraction of the cascade which intersects the surface, electrons might be emitted, provided their kinetic energy is in excess of the electrons' surface binding energy, $E_{sb,e}$. This surface barrier is determined by the work function, Φ_w, and the Fermi energy, E_F. For most clean metals the work function and the Fermi energy are of the order of $\Phi_w \approx 5$ eV, thus giving a surface barrier height of $E_{sb,e} \approx 10$ eV; for a more detailed discussion see Chap. 2.2.4.

By a formalism analogous to SIGMUND's, SCHOU (1980) arrived at an expression for the electron yield

$$\gamma = \Lambda_e \cdot F_{d,e}(x=0) \qquad (2.6)$$

where, in entire formal analogy to sputtering, Λ_e is a material parameter depending reciprocally on $E_{sb,e}$, and $F_{d,e}(x=0)$ is the average energy deposited into kinetic energy of electrons. Here too, the leading quantity is the stopping power hence giving

$$\gamma \propto E_{sb,e}^{-1} \cdot dE/dx)_{elec} \qquad (2.7)$$

This is the gist of BETHE's approach (1941). More

precisely, BETHE stated the electron yield to be proportional to the ratio of stopping powers of the projectile at the surface and the excited internal electron, respectively.

$$\gamma \propto dE/dx)^{p}_{elec} / dE/dx)^{e}_{elec} \qquad (2.8)$$

This global treatment of electron emission, which puts the physics of the excitation process into the stopping of the projectile, was extended later by STERNGLASS (1957) and others, and found its presently most elaborate form in SCHOU's (1980) cascade theory.

The dependence of the electronic and nuclear stopping power is shown in a schematic form in Fig.2.5. In order to appreciate their respective regions of dominance, it is convenient to consider scattering and stopping processes in a properly normalized, relative energy scale. Such a scaling has been introduced by LINDHARD and co-workers; it allows the treatment of stopping independent of the particular collision partners chosen from the periodic table. In this universal scheme, the energy parameter ε is

$$\varepsilon = \frac{a_L}{Z_1 Z_2 e^2} \cdot (E \frac{M_2}{M_1 + M_2}) \qquad (2.9)$$

where M_1 and Z_1 refer to the projectile's mass and atomic number, M_2 and Z_2 to those of the scattering atom (the target[2]), a_L is a screening length derived from the Thomas-Fermi atom

$$a_L = 0.88\, a_H\, [\, Z_1^{2/3} + Z_2^{2/3}\,]^{-1/2}, \qquad (2.10)$$

and $a_H = 5.29 \times 10^{-2}$ nm is BOHR's radius of the hydrogen atom.

The nuclear stopping power reaches its maximum at about $\varepsilon = 0.5$ and dominates for heavy projectiles up to $\varepsilon = 1$ and more. For Ne^+, Ar^+ and Xe^+ ions incident on copper, $\varepsilon = 1$ means, for example, laboratory energies of 45 keV, 110 keV and 715 keV, respectively. In the bombardment condition regime considered in this overview, we are therefore predominantly dealing with nuclear scattering and slowing down. In this regime, electron emission is always accompanied by pronounced atom emission.

Above $\varepsilon = 1$ elastic atom/atom scattering is of the Rutherford type; screening of the nuclear

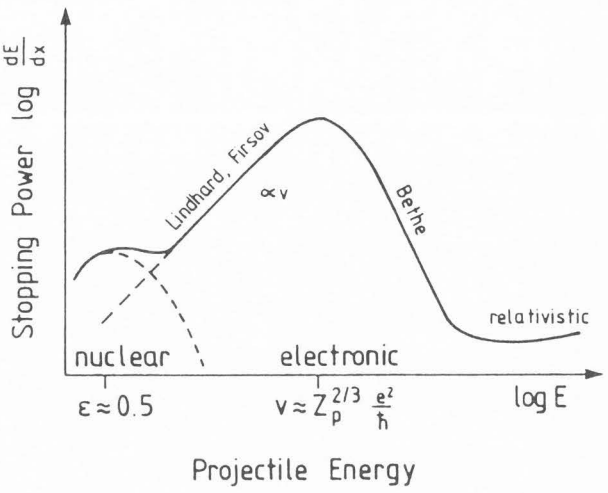

Fig. 2.5: Stopping power (schematic) of energetic ions as a function of energy.

charges is of minor importance for the elastic part of the collisions and the interaction is treated in the Coulomb-force field of the nuclei. Here, the nuclear stopping power is inversely proportional to the projectile energy. Consequently, the sputtering yield decreases also. Electronic stopping, on the other hand, rises monotonously with energy throughout this regime up to projectile velocities comparable to the orbit velocity of the projectile's electrons, which is

$$v = \frac{e^2}{\hbar} Z^{2/3} = v_H \cdot Z^{2/3} > 10^9 \text{ cm/s}.$$

$v_H = 2.2 \times 10^8$ cm/s is the Bohr velocity of the electron in the hydrogen atom. The generally used, if not accepted, dependence of electronic stopping is a friction-like proportionality to velocity

$$\left(\frac{dE}{dx}\right)_{elec} = k \cdot \sqrt{\varepsilon} \qquad (2.11)$$

with

$$k = 8 \times 10^{-2} \frac{Z_1^{2/3} Z_2^{1/2}}{(Z_1^{2/3} + Z_2^{2/3})} \cdot \frac{(M_1 + M_2)^{3/2}}{M_1^{3/2} M_2^{1/2}} \qquad (2.12)$$

At still higher velocities - in the Bethe regime - the projectile interacts with the bound electrons as in a point-charge collision. This is again a Coulomb-type collision, for which the stopping cross section decreases with increasing energy. In this regime, electronic stopping exceeds nuclear stopping by orders of magnitude. Here, the collisional emission of atoms is vanishingly small compared to electron

[2]The often-found notation of indices "1" for the projectile and "2" for the target is used here only when a specific collision is considered. Otherwise we prefer "p" for the projectile and "t" for the target.

emission.

In Fig.2.4 the electron yield of copper is shown as it varies with the energy of light and heavy projectiles, respectively. Only for the light ions is proportionality between γ and the electronic stopping power - or, more properly, the deposited electronic energy - is found, see HASSELKAMP and coworkers (1981, 1988). For heavier projectiles, Λ_e in Eq.2.6 loses its significance as a proportionality constant depending on the target only. In order to understand this difficulty, it is necessary to treat the electron emission phenomenon in a *microscopic* theory which specifically addresses the physics of the excitation mechanisms. Global theories, which lump all these processes into the stopping power, must fail when the processes contributing to electron emission and stopping, respectively, are of different weight in these two fields. This is the subject of the next chapter.

2.2.2 Excitation of internal electrons. The excitation of electrons in solids, i. e. the generation of electrons with kinetic energies above thermal equilibrium, can be accomplished by a variety of processes. These processes include

a) free-electron excitation by direct projectile/electron collisions;

b) free-electron excitation by plasmon decay following a collective electronic excitation by the projectile;

c) free-electron excitation in a "thermal spike" around the projectile's impact (thermionic emission);

d) core-electron excitation by inelastic Coulomb-like collisions;

e) core-electron excitation by electron promotion in atom/atom collisions.

All of these processes contribute to the slowing down of the projectile as well. Their combined action constitutes the electronic stopping power, $dE/dx)_{elec}$, of the target with respect to the incident radiation. The correlation between electron emission and electronic stopping, which is particularly clear in the high-velocity regime, was recognized 50 years ago. The first theories of particle-induced electron emission already followed this concept, BETHE (1941), STERNGLASS (1957). One should be aware, however, that, in order to achieve electron emission, the transferred energy must exceed the work function Φ_w. This requirement constitutes a severe selection of impact parameters and excitation mechanisms capable of electron emission. There are electronic stopping mechanisms which may, in a given velocity range, even dominate stopping, but which are sub-threshold

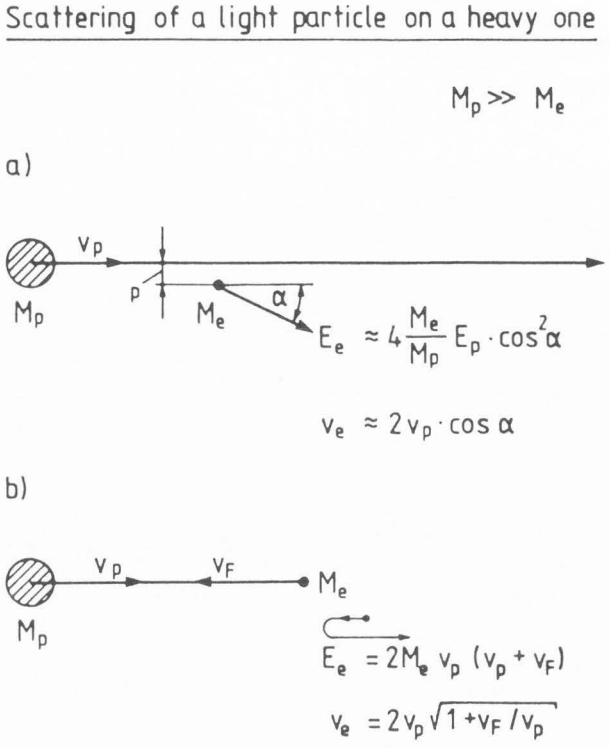

Fig. 2.6: Scattering of a light particle, here an electron of mass M_e, on a heavy one, M_p. In a), the light particle is at rest and interacts with M_p at an impact parameter p. In b) a head-on collision is sketched where, in addition, the two collision partners have opposite momentum direction.

events for electron emission. This is the case, for instance, for heavy-ion bombardment of metals at velocities $v_i < 10^{-8}$ cm/s, the range of interest in the present work. *Vice versa*, the mechanism responsible for electron emission in this velocity range is not of any weight for electronic stopping. Put bluntly, one may therefore say: *where there is electron emission, there is electronic stopping, but electronic stopping is not necessarily accompanied by electron emission.*

a. Free-electron excitation by direct projectile/electron collisions. It stands to reason that this mechanism applies to metal targets only. Only in metals is the free-electron density high enough ($> 10^{21} cm^{-3}$) to bring this collision probability into significance.

Conceiving of the projectile/free-electron collision as a classical two-particle collision (Fig.2.6), the transfer of kinetic energy is given by

$$E_e = E_{e,max} \cdot \cos^2\alpha \qquad (2.13)$$

where α is the angle between the trajectory of the hit particle (recoil) and the incident-projectile direction, and $E_{e,max}$ is the maximum transferable energy

$$E_{e,max} = 4\frac{M_p M_e}{(M_p+M_e)^2}E_p \approx 4\frac{M_e}{M_p}E_p = 2M_e v_p^2. \qquad (2.14)$$

Maximum energy transfer is attained in zero-impact-parameter collisions (head-on collisions, $\alpha=0$), where the recoiling electron moves in the same direction as the projectile. Owing to the huge mass-mismatch, the energy transfer in direct ion/electron collisions is very small, typically

$$E_{e,max} < 10^{-4} \cdot E_p \qquad (2.15)$$

The situation is slightly more favourable when the appreciable velocities of the free electrons are taken into account (Fig.2.6). For electrons with velocities at the Fermi-edge, $v_e = v_F$, and in the direction opposite to the projectile's velocity v_p, the maximum energy transfer is

$$E_{e,max} = 2M_e v_p(v_p+v_F) = (1+\frac{v_F}{v_p})\cdot E_{e,max}(v_e=0) \qquad (2.16)$$

With typical values of $v_F = 10^8$cm/s and $v_p = 10^7$cm/s, these selected electrons indeed have better chances of overcoming the surface barrier,

$$E_{e,max} \geq \Phi_w. \qquad (2.17)$$

With this condition, a velocity threshold for the incident particle can be calculated

$$v_{p,th} = 1/2\ v_F\ [(1 + \Phi_w/E_F)^{1/2} - 1]. \qquad (2.18)$$

below which electron emission is impossible by direct ion/electron interaction.

These zero-impact parameter collisions are very improbable. Moreover, they are strongly forward-directed, they drive the electron *into* the target. Electrons excited by such collisions require a great number of collisions with free electrons or with target ion cores in order to obtain the isotropic emission distribution found experimentally in the backward direction, cf. Chap.4.5. Since, furthermore, such randomizing collisions entail energy loss to the excited electrons, Equation (2.18) is hardly representative of the onset of emission by direct collisions of projectile ions with free electrons. It gives the lowest conceivable value for this excitation mechanism. Yet, electron emission is observed well below this threshold.

A crude order-of-magnitude estimate, pertinent to ion detection by detectors based on ion-to-electron conversion (cf.Chap. 3.4), may illustrate this situation: for most metals we can approximate in Eq. (2.18)

$$\Phi_w \approx E_F \text{ and } v_F \approx 10^8 \text{ cm/s}. \qquad (2.19)$$

This renders a (target- and projectile-independent) threshold velocity of

$$v_{p,th} \approx 0.2 \cdot v_F \approx 2\text{x}10^7 \text{ cm/s}. \qquad (2.20)$$

By inspection of Fig.2.2, for instance, it is realized that there is already appreciable electron emission at such high ion velocities. The real threshold is lower by a factor of four. Obviously, another excitation mechanism is at work in this velocity regime.

To convert to a more convenient energy scale, we use

$$v = 4.4 \times 10^7\sqrt{E/M} \qquad (2.21)$$

where v is in cm/s, E in keV, and the mass M in atomic mass units. For the minimum projectile energy we would get

$$E_{p,th} \approx M_p / 2\ . \qquad (2.22)$$

This is at great variance with reality: if direct collisional excitation of free electrons were the only ejection mechanism, we would not be able to detect ions heavier than neon (20 amu) with our standard particle detectors - even if we operated them at 10 keV. But we do detect atomic ions over the whole chart of the nuclides (300amu) and molecular ions up to 10 000 amu and more.

Obviously, free-electron excitation in direct **heavy-ion** collisions is a sub-threshold process for electron emission in the $v_p \leq 10^8$cm/s range. It is, on the other hand, considered to be the main electronic stopping mechanism in this velocity regime. Electron emission and electronic stopping are controlled by different mechanisms, and under such conditions Eqs. 2.6-2.8 cannot hold.

The situation is different, of course, with light

projectiles. Protons of 10 keV are well above threshold for direct free-electron emission. Since, furthermore, their prime electronic slowing-down is also by virtue of interactions with free electrons, proportionality between γ and $dE/dx)_{elec}$ can be expected. Indeed, HASSELKAMP and coworkers (1981 - 1988) confirmed Eq.2.6 for hydrogen ion bombardment over a large range of impact conditions. For all heavier projectile ions, however, the authors met complications in interpreting their yield data in terms of such a straightforward proportionality as expressed in Eqs.2.6 and 2.7.

There is another peculiarity with light ions, namely their high backscattering probability. For medium to heavy target atoms ($M_t > 50$ amu), 20 to 40 % of incident protons are backscattered from the interior of the target. In view of the strong anisotropy of the excitation process, collisions with these backscattered, now outward-directed projectiles should greatly enhance the electrons' chance of overcoming the surface barrier, Eq. 2.17. It is tempting to draw again a parallel to sputtering, where emission in light-ion bombardment is governed by the *backscattered* flux.

b. Free-electron excitation by plasmon decay. Metals are capable of plasma oscillations by virtue of the unconstrained movement of the electron gas with respect to the rigid lattice of ion cores. Any perturbation of charge neutrality will cause a shielding relocation of the mobile conduction electrons. This relocation establishes charge neutrality over distances larger than the Debye length.

The passage of charged particles constitutes such a perturbation. If this passage occurs at a speed much smaller than that of the electrons, the system reacts adiabatically to the injected charge and there will be neither electron excitation nor projectile slowing down by this process. If, however, the projectile is injected at a speed of the order of the Fermi velocity, quantized longitudinal oscillations are induced in the free-electron gas system. The energy of these plasmons, as they are called, is typically $\hbar\omega_p = 10 \pm 5$ eV. If plasmons decay near surfaces - which they prefer since the surface constitutes an imperfection to the ideal crystal - the energy transferred to electrons is well in excess of the work function and electron emission is feasible.

In ordinary metals, the Fermi velocity is of the order of 10^8 cm/s. This means that plasmons are expected to have little influence on electron emission in the energy/mass regime of interest here. To be more specific, a threshold velocity of $v_{p,min} = 2.6 \times 10^8$ cm/s was found by RÖSLER and BRAUER (1984), for plasmon-related electron emission from aluminum bombarded with H^+ ions. This result appears to be in good agreement with the dielectric theory of electronic stopping (LINDHARD and WINTER), where a threshold of $1.24 x v_H$ was given for Al.

RÖSLER and BRAUER (1984-1989) carried out a detailed theoretical investigation on the respective contributions of single free-electron excitation (Sect. a.), collective free-electron excitation, and core-electron excitation (Sect. d.) by proton irradiation. They note that "*the contribution of conduction electrons and electron excitation by plasmon decay play an overwhelming role compared to the contribution of core electrons*". By comparison with the theory of electronic stopping they also conclude that excitation of core electrons is far more important in stopping (of 20-800 keV H^+ in Al) than in electron emission - which is just another example of what has been said about the correlation between γ and $dE/dx)_{elec}$ in the introductory part to this chapter.

Experimentally, plasmon contributions have been identified in ion-induced electron emission by HASSELKAMP and SCHARMANN (1982). These authors found characteristic structures in the low-energy spectrum of electrons emitted from Al upon bombardment with H^+, He^+, and Ar^+ ions. The velocity of the Ar^+ ions was clearly below the aforementioned theoretical threshold, but the authors point out that plasmons can be generated by energetic *internal electrons* as well; it should be noted that the critical velocity for plasmon generation corresponds to an electron energy of about 30 eV. According to HASSELKAMP (personal communication) electrons ejected by plasmons which were generated by internal energetic electrons may perhaps be the explanation to "shoulders" in electron spectra not allocatable to Auger transitions; see, for instance, the early work of BENAZETH and coworkers.

As regards electron bombardment, plasmon processes are of prime importance, see RAETHER (1980), and any recent overview on electron energy loss spectroscopy (EELS). Plasmon contributions to electron emission are held to be significant but appear to be difficult to quantify, GANACHAUD and CAILLER (1979), SCHOU (1988), CAILLER (1990, this volume).

In **insulators**, there are no free electrons, at least not previous to the projectile impact; here, collective oscillations of valence electrons may lead to

characteristic energy losses of swift charged particles. The relevance of this energy-loss process to electron emission is unknown. However, heavy ions in the MeV range liberate - owing to their high ionization density - clouds of quasi-free electrons along their tracks in the solid. In the ensuing relaxation process, plasma oscillations take place which may give rise to particle emission, KRUEGER (1977). We mention this *plasma desorption* process more for the sake of completeness and curiosity rather than pertinence. The mechanism was proposed to explain emission phenomena associated with fission product bombardment (for a recent review, see for instance, WIEN (1989)); it is clearly beyond the scope of this overview - as are, apparently, all emission processes based on collective excitation.

c. Free-electron excitation in thermal spikes. Thermal emission of electrons from hot metal surfaces - also referred to as thermionic emission -is due to the transfer of energy in phonon/electron collisions. In this way, the enhanced kinetic energy of the thermally agitated lattice is coupled to the high-energy tail of the electrons' Fermi distribution.

Enhanced motion of the target atoms is also accomplished in nuclear collisions of energetic projectiles with target atoms. The lifetime of ordinary nuclear collision cascades is of the order of one lattice vibration and thus too short for a noticeable amount of energy to be transferred to the conduction electrons. Cascade lifetimes are higher by two orders of magnitude, however, in cascades of very high energy density (>1 eV/atom). Such cascades, in which the majority of atoms is in motion, are referred to as nuclear collision **spikes**, or - in the author's view less appropriately - thermal spikes. An established method of generating nuclear collision spikes is by heavy molecular bombardment at 10 to 100 keV. For some time it was held conceivable that during the comparatively long lifetime of a collision spike a fraction of the kinetic nuclear energy might be transferred to free electrons, causing hot-electron generation in the spike volume. This could enable some electrons to overcome the surface barrier in a process similar to thermionic emission. A hot electron gas could also result in a plasma-like state of the spike. Such a model - generally referred to as the local thermodynamic equilibrium (LTE) model - was extensively used in *secondary ion emission* long after it had been abandoned in electron emission.

The very first theoretical model developed for ion-induced electron emission was based on thermal

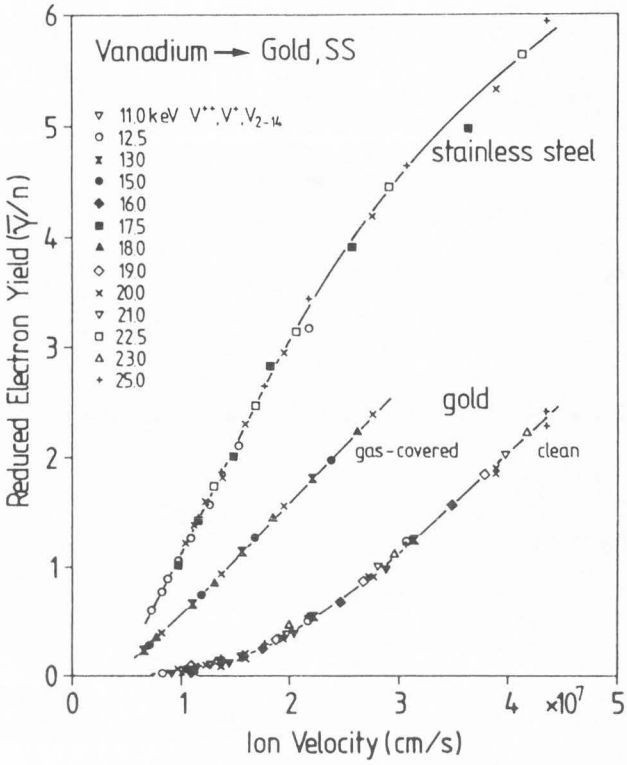

Fig. 2.7: Velocity dependence of the electron yield from a clean gold surface, from the same Au surface after air exposure, and from a technical stainless steel surface. Bombardment was carried out with vanadium atomic and cluster ions of energy 11 keV to 25 keV. In the case of cluster bombardment, the measured yield was divided by the number n of atoms in the cluster. Note that the γ/n versus v dependence is independent of n, no matter whether the dependence is linear (impure surfaces) in the threshold region, or more of the shape predicted by PARILIS-KISHINEVSKII (1960) (clean Au-surface). Unpublished results from THUM (1979), see also THUM and HOFER (1979).

emission, KAPITZA (1923). The Richardson-relation for the evaporation of free electrons was applied to a hot spot which was to be generated around the slowing-down region of the projectile. This theory was never accepted in the parameter range for which it was developed, namely for α-particles in the MeV range, BECKER (1924): near the surface, α-particles lose their energy by electronic interactions; nuclear collisions - the precondition to the development of a hot spot - come into play only at the very end of the range, far beyond the escape depth. KAPITZA's theory was found to be inappropriate, however, even for heavy projectiles, i.e., projectiles which generate high nuclear collision

densities, MORGULIS (1939), PAETOW and WALCHER (1938), PLOCH (1951). And it was finally rejected together with the mechanisms on which it bases when it turned out that even collision spikes showed no indication of thermionic emission components, THUM and HOFER (1979), VEJE (1981), SVENSSON et al. (1982).

This was concluded from measurements of the velocity dependence of the electron yield with cluster ions. The yield per atom in the cluster was found to be the same as that for atomic projectiles when compared at the same velocity. Also, the functional dependence of the yield was the same when the velocity was varied by either the energy or the mass (cluster size) of the cluster, see Fig. 2.7. Thus, for a given projectile/target combination the electron yield is solely a function of the *velocity* of the projectile, independent of whether or not the nuclear collision density is increased by the concurrent slowing down of cluster components in the cascade volume.

The physical reason for the absence of additional thermionic emission from nuclear collision spikes is that there is no spacial confinement of epithermal electrons within the volume of the spike. Since the mean free path length of an excited electron is of the same order as the spike's linear dimension, any small amount of energy an electron may pick up in a collision with recoiling atoms is quickly dissipated to the bulk. In fact, free electrons contribute to the cooling of nuclear collision spikes rather than being heated in, and evaporated from a small, confined volume. With respect to emission from spikes, electron emission thus shows quite a different, namely a linear, behaviour than the emission of atoms. (We note in passing that emission from spikes bears on still unsolved questions connected with ***molecular bombardment***). Deviations from linearity between the electron yield and the number of constituents in the molecule, and, moreover, the substantial emission below the projectile-velocity threshold have been repeatedly associated with spikes, see HOFER's (1980) overview, BEUHLER and FRIEDMAN (1980), BEUHLER (1983).

It should finally be noted that all these investigations pertain to metallic conductors. Ionization spikes in *insulators* may hold some unexpected results in store. The Richardson-equation, however, would be inappropriate all the same.

d. Core-electron excitation by point-charge collisions. As the name implies, point-charge collisions with atoms or ions refer to the impact of fully stripped ions and apply, therefore, mainly to proton and α particle irradiation. We shall only touch on this interaction, for two obvious reasons
- ionizing point-charge collisions are high-velocity events; minimum projectile velocities of the order of the electrons' orbital velocity, $Z^{2/3} \cdot v_H > 2.2 \times 10^8$cm/s, are required.
- this review focuses on multi-electron projectiles. For these projectiles, point-charge approximations cannot be made when *electronic* interactions are to be considered, see Sect. e.

The interested reader is referred to the reviews of GARCIA et al. (1973), SIGMUND (1975), and STOLTERFOHT (1987) for further information and full references to the authors mentioned in the following.

In the simplest models, the collision is regarded as a direct Coulomb interaction of the projectile with a bound electron. The initial state of the bound electron is represented by a hydrogenic wave function in the field of the screened nuclear charge (SLATER), the final state by a free electron and a ground state ion. The effect of the projectile is treated as a perturbation to the target atom. This can be done either in real space by applying the impulse approximation in various refinements (BLOCH, BANG and HANSTEEN), or in a quantum-mechanical treatment by using plane wave Born approximations (BETHE, HENNEBERG). Both treatments yield BETHE's well-known formula for the ionization cross section

$$\sigma_{io}(E) = C \cdot Z_t \cdot (E_p \cdot E_{io})^{-1} \cdot \ln \frac{E_p}{I} \quad (2.23)$$

where C is a calculable constant depending on the electron shell which is to be ionized with the ionization energy E_{io}, and I is the mean ionization potential of the atom.

Perturbation treatments meet their limitation at projectile energies near the ionization threshold, $E_p \approx E_{io}$. Abandoning staight-line projectile trajectories does improve agreement between experiment and theory, but this refinement does not solve the principal problem in the threshold regime. This problem lies in the fact that the collision time becomes large enough to allow the target electrons to accomodate to the passing charge.

A comparison of excitation by point-charge projectiles and electron-carrying projectiles, respectively, is shown in Fig. 2.8 in the case of beryllium K-shell ionization. Apparently, the Coulomb ionization by point charges is less effective by at least two orders of magnitude in the velocity range

of $< 10^8$cm/s. In this velocity range, the order of magnitudes of σ_I for the electronic shells of relevance in this overview is thus 10^{-20} to 10^{-19} cm^2 for Coulomb excitation, and 10^{-18} to 10^{-17} cm^2 for excitation by molecular orbital promotion in atom/atom collisions (Sec. e.).

It is important to note that in core-electron ionization the ionization energy may be lost for electron emission. This is the case when the electron hole created in the target's ion core relaxes by way of emission of quantum radiation and this radiation is not absorbed. Then, only the energy transferred to the electron in excess of the ionization energy is available for electron emission. The fraction of radiative to nonradiative transitions, generally referred to as ***fluorescence yield***, decreases with decreasing atomic number and with increasing principal quantum number of the excited atom. For K-shell vacancies, for instance, the two de-excitation channels have about equal probability for copper, i.e. the fluorescence yield of Cu K-shell vacancies is 0.5. This break-even shifts to higher atomic numbers for L, M, and higher-order shell vacancies. As we are dealing here mostly with outer-shell excitation, nonradiative de-excitation prevails in general under the conditions envisaged.

In nonradiative transitions - or Auger transitions, the two terms are synonymous - the energy released in de-excitation is transferred to another electron, which then carries away the energy difference of the two atomic shells concerned. This electron may come either from the target atom itself, or from one of the electron bands of the solid. In either case, an energetic electron is created which not only posesses enough energy to overcome the surface barrier but also may generate further electrons in cascade processes in the solid, Chap. 2.2.3.

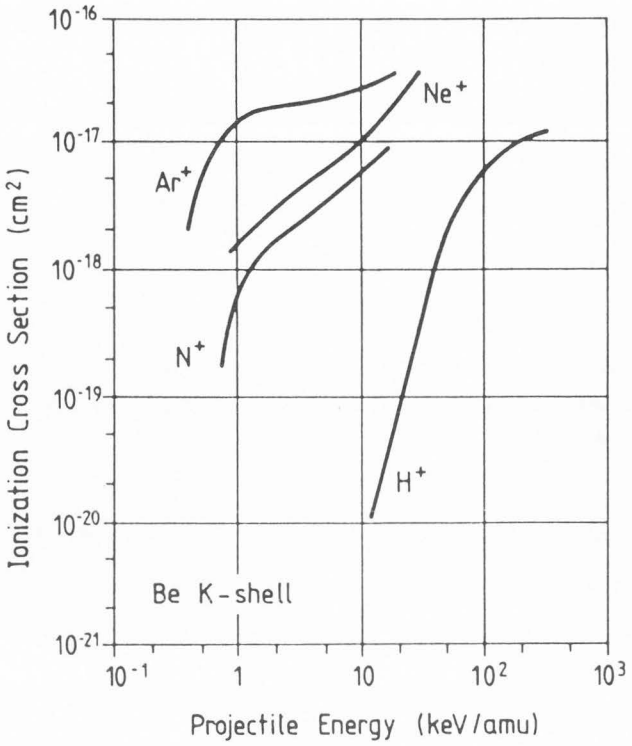

Fig. 2.8: Ionization cross section of the Be K-shell (E_{io} = 116 eV) for point-charge excitation (H^+), and excitation by multi-electron projectiles (N^+, Ne^+, Ar^+), respectively. K-shell excitation is not the most probable excitation of bound electrons in the context of this overview. But - apart from data availability -the Be K-shell energy corresponds, in order of magnitude, to the energies of outer-shell excitation relevant here; K-shell data of σ_I are also more reliable than those of M- and higher-order shells, mostly because of uncertainties of the fluorescence yield. Note that the data are given for equal velocity. According to Eq.2.21 10 keV/amu correspond to a velocity of 1.4×10^8 cm/s. Data from TARASAWA et al., see GARCIA et al.'s overview (1973).

e. Core-electron excitation by electron promotion in atom/atom collisions. Thus, all the excitation mechanisms discussed so far in Sec. a. to d. do not apply to heavy projectiles, or are sub-threshold processes for velocities below 10^8 cm/s. PLOCH (1950, 1951), in view of this dilemma and having just discovered the electronic shell effect on electron emission from solid targets (Chap.4.4), suggested one could understand the excitation in heavy-ion-induced electron emission by considering a mechanism proposed by WEIZEL and BEECK (1932).

BEECK and others, see his review of 1934 or the monography of MASSEY et al. (1974), had conducted extensive inelastic collision experiments on gas targets in the 100 to 500 eV energy regime. Sharp threshold energies for ionization and a pronounced electronic shell effect on the ionization cross section were found. Moreover, the onset of intensive ionization was determined to occur at projectile velocities which were two orders of magnitude smaller than electron orbital velocities. In the late 1920s, not even a sketch of a model existed which would have allowed the understanding of excitation in collisions where the electron orbitals could adapt themselves at any time of the collision to the projectile's force field; in this respect, these slow collisions are the direct

opposite to the BETHE-BLOCH perturbation conditions mentioned in the previous section.

In a collaboration with WEIZEL, BEECK interpreted this effect in the framework of the then newly-developed theory of molecular binding (HUND, MULLIKEN). They considered the collision partners during their time of interaction as a molecule of varying internuclear distance. Certain molecular orbitals become shifted to higher energies upon the approach of the nuclei and actually overlap or cross other electron energy levels. The $4f\sigma$ orbital was identified to be particularly prone to promotion to higher states. If electrons promoted to higher principal quantum numbers do not return to their original atomic orbital during the separation phase of the collision, an excited atom is left. By way of an autoionizing process the excited atom could be transformed into an ion and an energetic electron - so far WEIZEL and BEECK 1932. It took more than 30 years to refine this model of inelastic collisions of multi-electron projectiles, FANO and LICHTEN (1965); see the overviews of GARCIA et al. (1973) and LICHTEN (1980).

Electron excitation in heavy-ion-induced electron emission should be perceived as an Auger de-excitation process of atoms which have been excited in inelastic projectile/target-atom collisions. The particles involved are not only heavy in mass and thus ineffective in exciting free electrons, they also carry electrons. The interaction with the atoms in the target is, therefore, a multi-particle process, resulting in electron promotion to higher orbitals during the quasi-molecule phase of the interaction. The driving forces of electron promotion are the time-dependent two-center force fields of the nuclear charges and Pauli's exclusion principle. At and after the separation of the collision partners there is a finite chance for promoted electrons to remain in an excited level. The transition to the ground state follows then in about 10^{-14} s. For the outer electron shells this transition is predominantly of the nonradiative kind, i.e. the aforementioned Auger-process, cf. Chap. 2.1 and Fig. 2.1. Hence, in this model the (internally) emitted electrons originate from the conduction band while their energy stems from excited target and/or projectile atoms.

Unfortunately, but understandably, no theoretical treatment of this process exists which would allow to calculate the yield or any of its differential quantities. A major difficulty lies in the fact that the electronic transitions encountered in these comparatively low-energy collisions take place between outer energy levels. Very little is known about outer-shell ionization cross sections by heavy-ion impact, and the situation is even worse with fluorescence yields. Moreover, in solids the energy levels are broadened and the final states lie in the conduction band, Fig. 2.9. This renders the problem also material dependent.

In 1960, PARILIS and KISHINEVSKII published a theory of ion-induced electron emission which basically follows the above-outlined ideas on excitation of internal electrons, namely excitation of *bound* electrons followed by an Auger de-excitation process. The ion cores are regarded as Thomas-Fermi ions and their excitation is calculated much along the lines of FIRSOV's treatment of inelastic energy loss in atomic collisions. Electron transport to the surface and emission were treated in the usual manner, Chap. 2.2.3 and 2.2.4. It is obvious that this theory should find its main application under low-energy, heavy-ion bombardment conditions; the disregard of free-electron excitation excludes light projectiles as well as projectile velocities $>> 10^8$ cm/s, the Thomas-Fermi treatment prevents electronic-shell effects from being described in this scheme; BAKLITSKY and PARILIS (1972, 1986), tried to repair this latter deficiency by introducing Slater wave-functions.

The Parilis-Kishinevskii theory is the most often quoted theory in this field. It was praised in the first years after its appearance and has been seriously criticised in recent times, e.g., ALONSO et al. (1980), FERRON et al. (1981a), HASSELKAMP (1985). The theory is vague in parts of the derivation and contains some flaws which, when removed, increase disagreement with experiment. On the other hand, its results should not be taken too quantitatively, a confidence interval of 100 % is probably too narrow. Especially in the threshold regime care should be exercised, since not only are the threshold velocities too high by a factor of 2, but also the $\gamma \propto \arctan(v_p)$ shape of the yield curve is under dispute, e. g. COOK and BURTT (1975), FERRON et al. (1981a), THUM and HOFER (1979, 1984). In view of the complexity of the phenomenon of ion-induced electron emission, however, it is inappropriate to place the demands for quantitative accuracy too high. The theory can be regarded as successful if it reproduces the gross features of the phenomenon correctly. In the author's view, this is the case within the regime it aims at.

2.2.3. Transport to the surface. Electrons are excited by the projectile along a large part of its path length in the solid. Emission of these internally

liberated electrons is possible only if they reach the surface with an energy larger than the surface barrier. On their way to the surface, electrons experience collisions at the target's ion cores, lattice phonons, and the free electrons. Collisions, in which the heavy ion-core mass is involved lead primarily to scattering with little effect on the electrons' energy; high-resolution electron spectroscopy is required to identify this minute energy transfer. These collisions are important, however, in transforming anisotropic source distributions of excitation into the isotropic emission distribution observed experimentally, cf. Chap. 4.5.

Collisions with free electrons, on the contrary, strongly affect the energy of the excited electrons. In **metals**, where the free-electron density is of the order of 10^{22} cm^{-3} and more, this results in mean free path lengths as small as $\lambda = 1$ nm for electrons of energy $1 \leq E \leq 100$ eV. Thus, the electrons ejected are generally not the same ones as those excited by the projectile, but have received their momentum via an electron cascade. Only collisions within the escape depth and of proper momentum - both with respect to direction and amount - will lead to emission.

For metals, the ***escape depth*** λ_e is probably 2 to 5 times the mean free path length λ. The uncertainty stems both from diverging definitions and experimental difficulties. In **Auger electron spectroscopy**, for instance, the escape depth is determined by the mean free path length between collisions where a noticeable energy loss is encountered; noticeable means that the electron will no longer be recognized as an Auger electron after the collision. It has lost its discrete, characteristic energy and appears now in the broad spectrum of excited electrons. It would still contribute to the integral electron yield, however, should it make it across the surface barrier. Pure scattering events, on the other hand, are of relevance only if they result in large-angle deflections so that they remove the entire particle from the solid angle of acceptance (of the collector or the spectrometer). This example illustrates that in **electron emission**, this stringent definition of λ is of little relevance, since any electron leaving the surface will be identified as "emitted". λ and λ_e depend on the effect to be studied; see also SCHOU's comments in his overview of 1988.

With **metals**, the escape depth is thus assumed to extend over only a few monolayers. It is, therefore, in general smaller than the projectile's range or path length. Only in the threshold regime is this assumption questionable, especially when

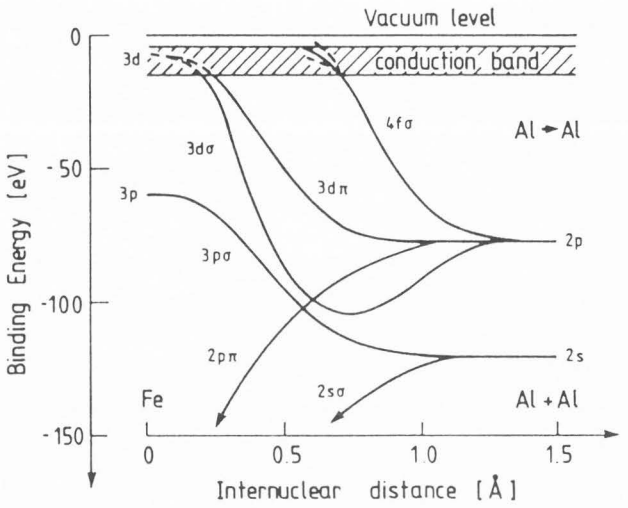

Fig. 2.9: Mechanism of generating 2p holes in Al by electron promotion into the conduction band. JOYES (1973, review). The collision is assumed to take place between an energetic Al atom (projectile or recoil) and an Al atom in metallic aluminum; Figure from WITTMAACK's review on secondary ion generation (1977).

low projectile energies and oblique incidence are combined. This appears to be the case in some fields of plasma-solids interaction, especially when magnetic fields are used for plasma confinement.

The free-electron density differs from metal to metal. An increase in the free-electron density results in a decrease of the escape depth and an increase of the stopping power. Accordingly, also the electron yield is affected in opposite directions. Such yield variations with the (metal) target material - also referred to as "Z_2-dependence" of the yield - are well known in secondary electron emission, BARUT (1954), MAKAROV and PETROV (1981). In ion-induced electron emission, this effect has been present latently in data compilations but was only recently demonstrated consistently by HIPPLER and coworkers (1988). These authors find an interpretation in terms of λ_e and $dE/dx)_{elec}$ still not entirely satisfying.

Binding free electrons by near-surface reactions with reactive gases, results in a decrease of energy-dissipative scattering centers, thus an increase of λ_e and, consequently, an increase in the number of electrons reaching the surface capable of overcoming the surface barrier. The yield rises in such cases, unless the surface reaction has increased the surface barrier as well. In general, the effect of alteration of the transport parameters λ, λ_e is stronger than that of the barrier height E_{sb}. This

trade-off between the influences of the escape depth and the work function has obscured interpretation of many of the older investigations; the incorrect explanation of the otherwise perfectly acceptable measurements of PAETOW and WALCHER (1938), for instance, is due to these counter-acting effects of surface layers or adsorbates.

The propagation of electron momentum and energy in cascades initiated by primary excitation events is the subject of transport theory. It has been treated analytically, numerically, and with the aid of Monte-Carlo simulation by a great number of workers since the mid-fifties. As we have stated in the introduction to this chapter, it is a transport-theoretical problem which is largely independent of the physics of the primary ionization. It will, for this reason, not be reviewed here; see WOLFF (1954), HACHENBERG and BRAUER (1959), RÖSLER and BRAUER (1981-1989), SCHOU (1980), DUBUS et al. (1987), BINDI et al. (1987).

In **insulators**, the situation is entirely different. The absence of free electrons as energy-dissipative scattering centers results in mean escape depths several orders of magnitudes larger than in metals. Or, to put it in BETHE's (1941) words: "*In insulators, the rate of energy loss of the secondaries is extremely small because they cannot give energy to electrons in the filled bands; hence the large secondary electron emission of insulators.*" Owing to this large escape depth, there is no such clear separation in space between electrons generated by primary ionization/excitation and those generated by cascade multiplication. Electrons from the primary event can very well be present in the emission spectrum. From the limited experimental material on insulators it must be said though, that there is no evidence of a dominance of this component. - The effect which is most obvious with insulators is the high integral electron yield. This is generally ascribed to the large escape depth. With λ_e extending from several 100 nm (typical) to 20 μm (exceptional, inert-gas layers GULLIKSON (1988)) the entire slowing down region of the projectile lies in the escape zone. Under such conditions, all the electron emission models based on the geometry sketched in Fig.2.3 become questionable. The interpretation of the incident-angle or the energy dependence of the yield given in Chap. 4.2 and 4.3, for instance, cannot be accepted for insulators without restrictions.

2.2.4. Emission from the surface. An electron excited in the solid can enter the vacuum continuum when its kinetic energy is large enough to overcome the potential barrier at the solid/vacuum interface. The physical nature of this barrier depends on the electronic structure of the target. Since it exerts a profound influence on low-energy emission - which, after all, constitutes more than 90 % of the total emission - the shape and height of the surface barrier require careful consideration. As there appears to be some confusion in the terminology, we first recall some of the physics involved in the different terms.

The situation is relatively clear with **metals** where, by definition, the ***work function*** is the minimum energy required to remove an electron from the solid. This energy, Φ_w, is determined by the distance of the Fermi-edge to the continuum, cf. Fig. 2.1. As long as the surface barrier is discussed in terms of the energy *transferred* to the electron, the work function can be regarded as the the barrier height - undoubtedly a convenient and pertinent measure. Since it is customary, however, to use the bottom of the conduction band as reference for internal kinetic energies, the surface barrier in this frame is

$$E_{sb} = E_F + \Phi_w. \qquad (2.24)$$

Here the *total* kinetic energy of the excited electrons is addressed. Unfortunately, in **semiconductors** the work required to move an electron from the solid to the vacuum is also referred to as ***electron affinity***, while the work function still is used to mark the distance of the Fermi edge from the vacuum continuum. The Fermi edge lies in the band gap of these solids and is thus meaningless for electron emission. In this definition with semiconductors, the electron affinity is the surface barrier. It is temperature and dopant dependent.

With **insulators**, the situation appears to be unambiguous. It is the electron affinity which sets the surface barrier for electron emission. In a first approximation, atomic ionization energies can be used for E_{sb}; to give an example, the respective numbers for solid xenon are: E_{sb} = 9.7 eV, E_{io} = 9.3 eV.

The classical work-function-type barrier is a *planar* surface barrier. It has been used as such paradigmatically in other fields of particle emission, most notably in sputtering. There too, a surface barrier of some electron volts influences critically the low-energy flux of emitted atoms. A planar surface barrier means that during the electron's egress from the surface a force perpendicular to the surface acts on the particle. This force leaves the

tangential momentum component unchanged

$$p_{in} \cdot \sin \theta_{in} = p \cdot \sin \theta \,, \qquad (2.25)$$

while it removes from the internally available kinetic energy, E_{in}, an amount equivalent to the barrier height

$$E = E_{in} - E_{sb} \,. \qquad (2.26)$$

The quantities E, p, and θ refer to the ejected electron's energy, momentum and polar angle, respectively. These are the quantities accessible to the experiment, while the corresponding quantities inside the surface - marked with the index "in" - must be calculated from transport theory or inferred from numerical simulation. They can be inferred from the energy and angular distribution of emitted electrons also, but this requires exact knowledge of the surface barrier.

The reduction of only the normal momentum component at the electron's exit from the solid causes a refractive effect on the electron trajectory which is analogous to light refraction at the transition to an optically less dense medium. The change of polar angles follows directly from Eqs. 2.25, 2.26 and is given by

$$\sin \theta = \sin \theta_{in} \sqrt{1 + \frac{E_{sb}}{E}} \qquad (2.27)$$

The exit polar angle, therefore, always exceeds the polar angle under which the internal electron arrives at the surface, and for every internal energy a certain exit cone exists, beyond which "total reflection" of the electron at the surface occurs. This limiting angle for θ_{in} follows directly from Eq. 2.27 with $\theta = \pi/2$

$$\sin \theta_{in} = \sqrt{1 - \frac{E_{sb}}{E_{in}}}, \qquad (2.28)$$

according to which the opening angle of the exit cone shrinks to zero at $E_{in} \approx E_{sb}$. The most important consequence of this is that the energy spectrum of ejected electrons deviates markedly from that of internal electrons: let $N_{in}(x,E_{in},\Omega_{in})\, dE_{in}\, d\Omega_{in}$ be the number density of internal electrons in the intervals $(E_{in}, E_{in}+dE_{in})$, $(\Omega_{in}, \Omega_{in}+d\Omega_{in})$ at the depth x from the solid's surface. $N_{in}(x, E_{in},\Omega_{in})$ is the distribution function which follows from solving the Boltzmann equation. The corresponding flux density then is

$$j_{in}(x,E_{in},\Omega_{in}) = N_{in}(x,E_{in},\Omega_{in}) \cdot v_{in} \cos \theta_{in} \qquad (2.29a)$$

and at the surface $x = 0$

$$j_{in}(0,E_{in},\Omega_{in}) \equiv j_{in}(E_{in},\Omega_{in}) = N_{in}(E_{in},\Omega_{in}) \cdot v_{in} \cos \theta_{in} \qquad (2.29b)$$

Particle conservation at the solid/vacuum transition requires

$$j_{in}(E_{in},\Omega_{in})\, dE_{in}\, d\Omega_{in} = j(E,\Omega)\, dE\, d\Omega \qquad (2.30)$$

which gives with $dE_{in} = dE$, and differentiation of Eq. 2.27

$$j(E,\Omega) = j_{in}(E_{in},\Omega_{in}) \frac{E}{E+E_{sb}} \cdot \frac{\cos\theta}{\cos\theta_{in}} \qquad (2.31)$$

It is obvious that the transformation factors to the internal flux distribution on the right hand side of Eq. 2.31 result in significant deviations of the emitted distribution from j_{in}. This is particularly clear with the energy spectrum, where the transformation causes the emitted spectrum to start at the origin and run through a maximum before it approaches the internal distribution at high energies. This internal spectrum, on the other hand, is generally assumed to be of a monotonously decreasing shape such as, for instance, a $1/E_{in}^2$ distribution. We will resume this discussion in the pertinent chapters on energy and angular distribution.

A planar surface barrier is certainly a good approximation for the emission from metal surfaces. With metals, the barrier is established by both the electric double layer caused by the spill-over of conduction electrons across the positive ion-core boundary, and the image force an electron creates during its dwell-time just outside the surface. Both components result in forces perpendicular to the surface equipotential plane. Care should be exercised when this model is transferred to insulators, however. We are not aware of specific investigations on this problem and would, therefore, restrict ourselves to indicating that the mechanism of ionizing atoms in non-conducting substances does not involve the surface at all. Should it turn out that also polarization effects are of little influence on the escape probability of excited electrons, a rotationally symmetric barrier would be more appropriate. In this case the same problems with energy spectra arise as have puzzled the sputtering community for the last 20 years. Owing to the scarcity of quantitative information on differential yields from insulators, it is clearly too early to enter this discussion in any more detail.

3. Notes on Experimental Techniques

3.1 Target Preparation and Vacuum Requirements

For 50 years following FÜCHTBAUER's work, virtually every publication on ion-induced electron emission noted the profound influence on the electron yield of sorbed gases in the target and of residual gases in the target chamber. This influence is very much stronger than for the emission of atoms by energetic particle bombardment. For this reason, in electron emission investigations the vacuum, the ion beam, and the target conditions usually stayed in the forefront of the respective techniques: in-situ degassing, flash desorption, differential pumping, liquid-N_2, trapping, and mass-separated ion beams were introduced already in the 1930's, OLIPHANT (1930), SCHNEIDER (1931), HEALEA et al. (1936, 1939), PAETOW and WALCHER (1938); also, the UHV technique was applied in ion-induced electron emission as soon as it was technically feasible, e.g., HAGSTRUM (1954a, b), PARKER (1954), MAHADEVAN et al. (1963, 1965).

All these complications are present in secondary electron emission as well. There is one advantage though, which workers in ion-induced electron emission appreciate when conducting their experiments: the ion beam can be used to clean the target surface. Carried out with care and an understanding of the sputtering process, this can be a very efficient *in-situ* cleaning procedure. The Figures 3.1 and 4.2 show examples of the effect of sputter cleaning in the case of targets which are notoriously difficult to prepare to an atomically clean surface state.

The importance of proper target preparation can also be appreciated from Fig. 2.7: exposure of a clean Au surface to air for several minutes contaminated the target in such a way that not only the amount of the yields but the whole yield dependence was altered. The clean-metal velocity-dependence of the yield comes much nearer to the theoretical result than the linear $\gamma(v)$-dependence observed for gas-covered surfaces. Once the surfaces were contaminated, THUM (1979) found it impossible to reach again the clean state by a baking procedure alone. A fresh layer had to be deposited on the target surface by *in-situ* evaporation. The electron yields obtained from surfaces prepared in this way are, in general, in good agreement with those of sputter-cleaned surfaces (FERGUSON 1987).

3.2 Integral and Differential Yields

The principles of the experimental method of measuring the yield and angular distribution have not changed very much since FÜCHTBAUER (1906a,b). The *integral yield* γ is usually determined by measuring two currents: either the currents to the target and to an electron collector around the target, or the currents to the target with and without an electron-suppression voltage. Variation of the bias voltage of collectors also provides information on the *energy distribution*, $d\gamma/dE$, via differentiation of retardation curves. *Angular distributions*, $d\gamma/d\Omega$, are similarly straightforward to obtain by an arrangement of collectors subtending small solid angles with respect to the beam spot at the target, cf. Fig. 1a. Angular and energy distribution data are also referred to as (single) differential yields.

Integral electron yields can also be measured with ion-electron converters (IECs). IECs not only allow the use of extremely small ion currents and fluences - thus avoiding beam-induced artefacts - they also render entirely new information, namely the emission statistics of electron emission. For this reason they will be dealt with in a separate chapter (3.4).

Double-differential quantities, such as the energy-resolved angular distribution or the angle-resolved energy distribution of emitted electrons are very difficult to measure with ion beams owing to the artefacts discussed in Chapter 3.3. The difference between these two quantities comes from where the instrumental compromise with respect to resolution in one variable is made in order to allow higher precision to the other: energy-resolved angular distributions are usually recorded with moderate energy resolution, and energy distributions measured with electrostatic condenser spectrometers are *per se* selective in space, i.e. angle resolved, owing to their small solid angle of acceptance (typically $\Delta\Omega < 10^{-2}$ sterad). Such angular-resolved energy distributions not necessarily yield the same kind of information as spherical retardation spectrometers do with their large acceptance of $\Delta\Omega \approx 2\pi$ (HASSELKAMP and SCHARMANN 1982). While the latter provide information on emission into the whole half-space above the surface, the former give insight in emission in specific ejection directions. By a judicious choice of impact and emission directions, specific excitation and ejection processes can be studied: SOSZKA et al. (1983, 1989) and BUDZIOCH et al. (1986), for instance, used this technique to study the emission of electrons after small-impact parameter collisions with atoms in the surface layer, and NEGRE et al. (1985) analyzed

asymmetries in the emission of Auger electrons from single crystals.

In energy-resolved angular distribution investigations, on the other hand, the sectioned hemispherical retarding-potential analyzer of MISCHLER et al. (1986) seems to be a very suitable instrument. Although it provides only moderate energy resolution, its polar-angle resolution is well acceptable, in particular in view of the need to find a compromise to keep beam induced surface structure changes at a tolerable level. Analyzers of this kind also allow the determination of single-differential and integral yields.

All methods of determining integral and differential yields require negligible secondary ion currents to and from the collectors. Secondary ions falsify the current readings and may, furthermore, induce electron emission from the collector and beam-defining diaphragms. Secondary ion emission is negligible for clean metallic surfaces, but care must be exercised with compound or insulator targets, or when the influence of reactive-gas coverages is to be investigated. Then the secondary ion yield changes even more with surface composition than the electron yield, see e.g. HOFER's review (1987) and references therein.

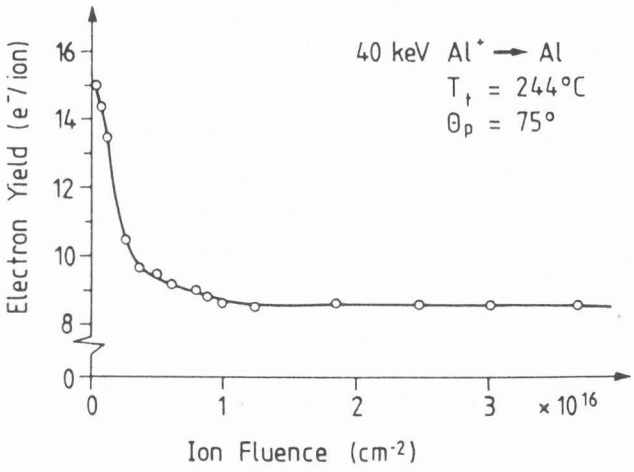

Fig. 3.1: Effect of cleaning by sputtering with "self"-ions. The target was kept at a temperature of 244 °C while bombarded under an angle of incidence of $\vartheta_i = 75°$; both measures reduce the likelihood of building up irradiation-induced surface structures. The electron yield saturates after removal of about 50 monolayers. From SVENSSON and HOLMEN (1981).

3.3. Ion Beam Induced Artefacts

The incident particle beam can profoundly influence the emission data. This is due to:

- changes of the surface morphology owing to sputtering, and
- changes of the chemical composition of the surface.

A particularly worrysome case is alkali-ion bombardment, because of the large effect of the implanted ions on the work-function. For this reason, alkali ion beams are no longer in use for fundamental investigations on ion-induced electron emission - despite the fact that much higher current measuring sensitivities are nowadays achievable; the fluence required for γ-determinations, for instance, has been reduced to less than 10^{-15} ions/cm^2. The issue gets new actuality, however, by the frequent use of liquid metal (Ga^+, In^+, Cs^+ etc.) ion sources in applications such as sub-micron imaging, analysis and processing of surfaces.

Fundamental research is generally carried out with inert-gas ions or "self-ions" ($Z_t = Z_p$). Also, the use of the ion-electron converter technique for measuring the integral yield and the emission statistics allows to overcome the problem of beam-induced artefacts, cf. Chap.3.4 and 4.7.

While for straightforward yield measurements the ion fluence can be kept sufficiently small, this may not be the case for the corresponding differential quantities $d\gamma/d\Omega$, the angular distribution, and $d\gamma/dE$, the energy distribution. And it clearly is not the case for double-differential quantities such as the energy-resolved angular distribution $d^2\gamma/d\Omega dE$. During the measurement of such highly selective processes the development of beam-induced surface structures on the target can hardly be circumvented. Their influence on electron emission - in particular on the polar angular distribution - has found its clearset demonstration in the work of the Toulouse group (MISCHLER et al. 1984, 1986, NEGRE et al. 1985, BANOUNI et al. 1985, MISCHLER and BENAZETH in their review of 1986, MISCHLER et al (1989)).

It appears that ion-induced electron emission investigations are running into the same surface-morphology problems as did sputtering about 10 years earlier, LITTMARK and HOFER (1978). Striking similarities exist between the dependence on surface morphology of the electron and atom emission yields, respectively. They are evident in angular-differential yields but can be seen in integral yield data also. In their comprehensive study of surface topography effects in electron emission, MISCHLER et al. (1986) indicate that the electron yield of "textured" surfaces is always higher than

that of flat surfaces[4]. In sputtering, this result was predicted and documented by LITTMARK and HOFER (1978); transferred to electron emission, their explanation was: under cascade emission conditions, the yield increase due to the higher effective angle of incidence (Chap.4.3) on structured surfaces exceeds the yield decrease due to recapture of emitted particles on these structures.

Surface structures affect the angular distribution of emitted electrons and atoms much in the same way; resemblances can be seen even in details of the emission characteristics. There is one peculiarity in electron emission, however, which has no equivalent in atom emission: the emission of Auger electrons from sputtered atoms decaying just outside the surface. For this radiation, MISCHLER et al. (1986) found an isotropic emission distribution which is even stronger altered by surface structures than the cosine-shaped emission characteristic corresponding to the electron flux emerging from inside the solid.

If no other means of eliminating morphology changes of the surface can be found, one may in investigations of target-independent emission characteristics have recourse to semiconductor targets. Semiconductors amorphize under room-temperature bombardment at heavy-ion fluences of about 10^{14} cm^{-2}. Such surfaces are less prone to develop facets, ridges, pyramides, cones etc. on the surface of ion-irradiated solids.

Recent reviews on structural changes due to energetic ion beams and the sputter-erosion they cause: KIRIAKIDIS et al. (1986), and the articles by CARTER et al. and SCHERZER in the monography on sputtering edited by BEHRISCH, Vol.2 (1983).

3.4 Ion-Electron Converters

In the 1970's, an entirely new technique was developed for determining the electron yield. This technique is based on the use of high energy-resolution detectors for electrons in ion-electron converters (IECs) and has profound advantages over the standard current-measurement methods. The conceptual design of IECs is shown and explained in Fig.3.2. The information provided is, in the first place, the ***emission statistics*** - which costitutes a unique possibility in the field of radiation-induced particle emission from solids. From the emission statistics the yield follows by fitting a probability distribution to the experimental data.

As **particle detectors**, IEC's were introduced by SCHÜTZE and BERNHARD in 1956; in this capacity they are in wide use now, e.g. DALY (1960), WERNER and DE GREFTE (1965), BLAUTH et al. (1971), STAUDENMAIER et al. (1976), HOFER and THUM (1978), RUDAT and MORRISON (1978), HEDIN et al. (1987). Their advantages lie in a high dynamic range, excellent time and load stability, fewer counting losses for heavy ions, and detection limits at ion currents of the order of 10^{-21} A.

The potential application of IECs in **ion-induced electron emission research** was recognized early, see the reviews of KREBS (1968, 1983), but their breakthrough came only when low-noise semiconductor detectors became available. The advantage of using IECs in ion-induced electron emission stem from the possibility of:

- using only very low ion currents ($< 10^{-15}$ A). Thereby, virtually every beam-induced surface alteration is eliminated and electric charging of insulating surface layers greatly reduced. Moreover, it enables the bombardment with ions which cannot be produced at beam currents high enough for standard current measurements; working with very low ion currents not only expands the range of usable atomic ions, it also opens up the field for molecular and cluster ion bombardment;
- resolving multi-electron emission. This allows the determination of the probability distribution of electron emission.

This possibility of measuring the emission statistics of the phenomenon is achieved with semiconductor detectors operated as low-noise, high energy-resolution (ΔE = 3-5 keV) electron detectors. The time-resolution is kept moderate ($\Delta t > 10^{-10}$ s), thereby allowing all electrons ejected as a consequence of one ion-impact to be registered in one output pulse; the height of this pulse is an integer multiple of the pulse height of a one-electron emission event (γ = 1). The pulse height distribution of an IEC equipped with such an electron detector thus consists of a set of discrete, equi-distant lines, their width being determined by the detector resolution, and their distance by the potential difference between the detector and the target (with IEC's, the target is usually termed conversion electrode). With the aid of a pulse height analyzer the frequency distribution of emission of a given number γ = 1, 2, 3, ... of electrons can be registered directly; an example of such an emission distribution is shown in Fig.3.3 for the case of bombardment of an Ag surface with 20 keV Si^+ ions. To this emission distribution a probability function $P(\gamma;\bar{\gamma},b)$ can

[4]This enhancement in the yield was found for both the intergal yield (the background in their experiments) and the Auger electron yield. Experimental conditions: 25 - 40 keV Ar^+, $Xe^+ \rightarrow$ Al.

Ion Electron Converters

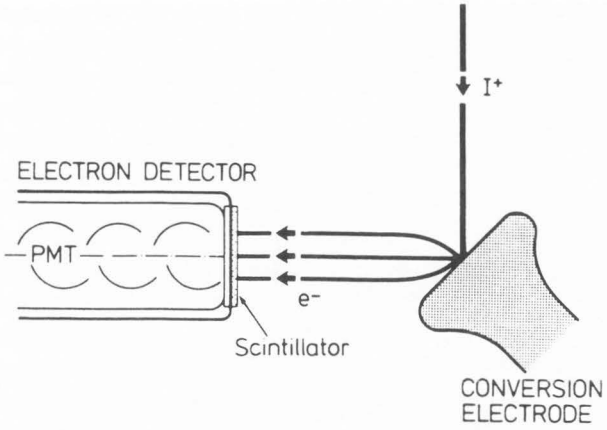

Standard Converter

Schütze & Bernhard 1956
Daly 1960

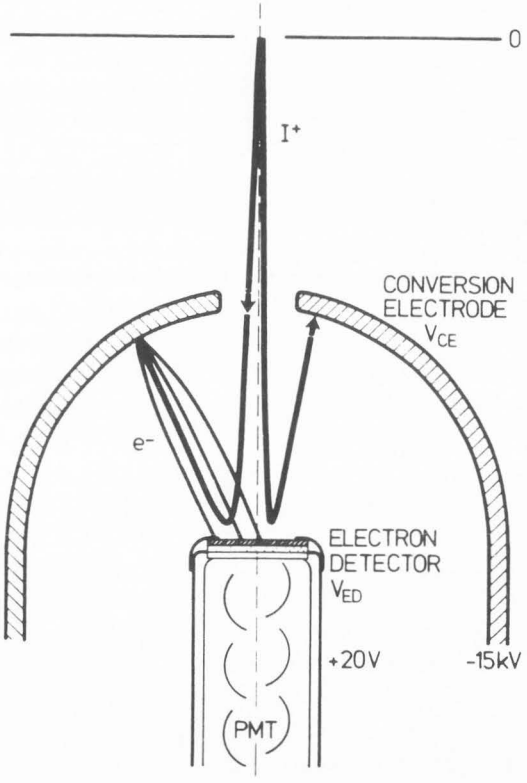

Mirror Converter

Daly et al 1968
Hofer & Kirschner 1974

Fig. 3.2: Ion-electron converters. In the versions shown here, the converters are equipped with scintillation counters for detection of electrons released from the conversion electrode. When used for fundamental studies on electron emission, it is advantageous to replace these detectors by high-resolution semiconductor detectors.

a. Standard IEC as developed by SCHÜTZE and BERNHARD (1956). As in conventional multiplier-detectors, the ions to be detected are converted into electrons and these electrons are multiplied with the help of a cascade of dynodes. With IEC's, however, a high ion-to-electron conversion efficiency is achieved not by means of surface chemistry ("activation" of dynodes), but by high ion energies: the conversion electrode of IECs is usually operated at a potential of -15 kV and more. This yields much better detection sensitivities for heavy ions as well as better ion-load and vacuum stability. The latter advantage is further improved by performing the electron-multiplication process in the separated vacuum of a photomultiplier tube (PMT); to this end, the electrons are converted into photons with the help of a thin scintillating layer on top of the PMT. Such IEC's are ideal positive-ion detectors, e.g. DALY (1960), but they can be used for electron emissiown studies as well, KREBS et al. (1968,1983), DIETZ and SHEFFIELD (1973), BEUHLER and FRIEDMAN (1977a).

b. Spherical mirror converter as developed by HOFER and KIRSCHNER. Here, the ions to be detected are electrostatically reflected in front of the electron detector; the electrons released from the conversion electrode are focussed on the electron detector in the very same electrostatic field. This converter is particularly suited for electron emission investigations as it provides inherent total electron collection.

---

be fitted, where $\bar{\gamma}$ and b are fitting parameters which will be discussed in detail in Chap.4.7. More often than not, a Poisson distribution is used

$$P(\gamma;\bar{\gamma}) = \frac{\bar{\gamma}^{\gamma}}{\gamma!} e^{-\bar{\gamma}}. \qquad (3.1)$$

The mean $\bar{\gamma}$, which is here equal to the variance, is the only fitting parameter available for this one-parameter distribution. $\bar{\gamma}$ is the conventionally

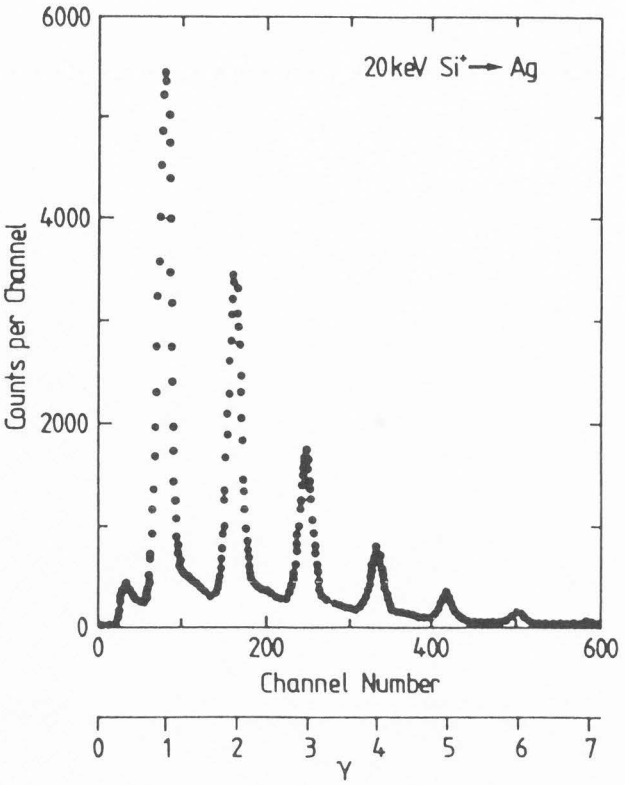

Fig. 3.3: Pulse-height distribution generated by a high-resolution ion-implanted silicon detector in an IEC of the type sketched in Fig. 3.2b. This as-registered spectrum reflects to a large degree the electron emission statistics, here that of electrons emitted from a clean Ag surface bombarded with 20 keV Si^+ ions at normal incidence. By fitting a Poisson distribution to this spectrum, an average electron yield of $\bar{\gamma}$ = 1.1 e^-/ion is obtained. From FERGUSON (1987).

determined (average[5]) electron yield, i.e. the number of electrons emitted per ion, averaged over a great number of ion impacts. $P(\gamma;\bar{\gamma})$ or, more generally, $P(\gamma;\bar{\gamma},b)$ thus provide the probability of emission of a given number γ of electrons *per individual projectile impact*, or, in other words, it provides the probability of zero-, single-, and multi-electron emission per individual collision cascade initiated by the projectile in the target.

There are several experimental and systematical difficulties to cope with:

- an experimental precondition for applications of IECs in ion-induced electron emission research is complete collection of emitted electrons at the electron detector. As the yield is derived from the measured emission statistics, it is mandatory that every emission event be recorded with the same probability. This requires either a special electron-optical transfer system (DIETZ and SHEFFIELD (1973), BEUHLER and FRIEDMANN (1977a), LAKITS et al. (1989a,b), or the use of the somewhat unwieldy but collection-efficient spherical mirror converter shown in Fig.3.2b (HOFER and LITTMARK, 1976, STAUDENMAIER et al., 1976, THUM and HOFER, 1979, 1984, FERGUSON and HOFER, 1989). Still, in investigations of the emission statistics, the small acceptance area of high-resolution semiconductor detectors may constitute a problem in discrimination-free electron registration.

- more than in current-measuring methods it is essential that electrons emitted by stray particles, such as ions, charge-exchange neutrals, and electrons, are prevented from registration; otherwise, the emission distribution is distorted and the average yield derived thereof strongly falsified.

- for the same reason, the loss of electrons from the detector by way of backscattering must be avoided. With standard IECs (set-up of Fig.3.2a), this is tried with magnetic fields (DIETZ and SHEFFIELD, 1973), in mirror converters the electrostatic mirror field itself takes care of the reversal of backscattered-electron trajectories. Still, these electrons loose a fraction of their initial energy in the dead layer of the detector surface, and this causes an asymmetric line broadening in the spectra (v. ASSELT et al., 1978). Although recognized since the pioneering work of DIETZ and SHEFFIELD (1973, 1975), it seems that the effect of backscattered electrons has been taken care of properly only recently (LAKITS and coworkers, 1989a, b).

- since the emission distributions turn out to be only approximately Poissonian, cf. Chap. 4.7, there is some uncertainty in determining $\bar{\gamma}$ via the emission distribution when the yield is small: in cases where $\bar{\gamma} < 1$ e^-/ion, too few $\gamma > 1$ events are available for establishing $P(\gamma;\bar{\gamma})$ with good accuracy; it is important to visualize in this context that the zero-emission event is not accessible to the measurement with this technique, i.e. $P(0;\bar{\gamma})$ must be deduced from the fitted probability function.

In the low-yield regime, where $P(0;\bar{\gamma})$ may be as large as 0.5, the converter method is, thus, not so much a precision technique for obtaining $\bar{\gamma}$, but rather a method of obtaining data otherwise not

[5] In a strict sense, all yields mentioned so far ought to be denoted as $\bar{\gamma}$ since they are average quantities. We have abstained from this notation here, however, since probability distributions constitute only a minor part in this overview.

accessible. Typical examples of this situation are the:

- electron-yield investigations by cluster-ion impact, touched on in connection with thermal emission in Chap. 2.2.2c, and the
- $\bar{\gamma}(Z_p)$-oscillations, viz. the dependence of the yield on the electronic shell structure of the projectile, discussed in Chap.4.4.

In the communications of which these examples were chosen it is also shown that the error in $\bar{\gamma}$-determinations with the IEC method is well acceptable. Typically it does not exceed 20 %. The accuracy-problem is more stringent when an unambiguous identification of the fundamental emission statistics is to be made. This attempt requires, first of all, a clear assessment of instrumental influences on the recorded frequency distribution as well as of the accuracy of the deconvolution procedure. Then a (Poisson-, Polya-, Binomial-, etc.) probability function can be fitted and the significance of the fit be tested. In the last step, the physical justification for the resulting probability function needs to be given. From the few investigations published as yet, it appears that a Poisson distribution is acceptable in many cases.

An interesting combination of the conventional and the converter method of determining the yield was carried out by LAKITS and coworkers (1989a, b, c): By replacing the electron detector by an electron collector and increasing the ion current by several orders of magnitude, the yield could also be determined by a straightforward measurement of the ion and the electron currents, i.e., without the need to fit a probability function to the measured frequency distribution. In this way, the reliability of not only the $\bar{\gamma}$ measurement cold be tested but also that of the assumed probability function.

4. The Characteristics of Ion-Induced Electron Emission

4.1. The Influence of Sorbed Gases and Altered Surface Layers

There is a widespread tendency to discard data obtained in the pre-UHVera. This is not always justifiable. As regards the integral yields, it is important that the targets were thoroughly degassed, Fig.2.7. Otherwise, the yields are not characteristic of the target element; they are generally also significantly larger than with degassed targets, PAETOW and WALCHER (1938), ALLEN (1939), HILL et al. (1939), BRUNEE (1957). It appears that in the regime of kinetic electron emission every step towards cleaner surfaces reduces the yield. This is a well-known fact also in secondary electron and secondary ion emission, see the review by SEILER (1982) and references therein.

However, where degassing was achieved - and this is the case for most of the work from 1930 onwards - there is hardly any more good reason for rejecting data obtained in the pressure range of 10^{-7} to 10^{-9} mbar, e.g., PLOCH (1951), BRUNNEE (1957), KLEIN (1965). It is certainly true that many of these data have not been obtained on atomically clean surfaces. This must not mean, however, that the yields are not characteristic of the target element. Recent work has shown that the effect of impurities like H_2, N_2, O_2 is much smaller when their presence is confined to the very surface than when they are bound in a target region extending over the escape depth λ_e, see e.g. FERRON et al. (1982), FERGUSON (1987). The presumed reason is that *adsorbed surface impurities* influence primarily the work function. Work function alterations are comparatively small for O_2, N_2 and H_2 adsorbed on metal sufaces. These impurities, when *bound in the bulk* on the other hand, not only affect Φ_w, they also change the excitation of internal electrons and, most importantly, increase their transport to the surface. As was discussed in Chap. 2.2.2, the electron transport is governed in metals by the free-electron density; this density decreases when metals form oxides, hydrides, nitrides, etc. Accordingly, the escape depth increases and so does the electron yield. The understanding of the whole phenomenon of the influence of impurities and composition changes was considerably hampered by a lack of distinction between surface adsorbates on the one hand, and altered layers of a thickness comparable to or exceeding the escape depth on the other, see e.g., PAETOW and WALCHER (1938).

Of comparatively reduced complexity is the role of adsorbed surface layers. Adsorbates on the surface proper may influence the yield by way of:

- alteration of the work function; this is qualitatively understood and extensively studied in secondary electron emission, see e. g. PALMBERG (1967), SCHAEFER and HOELZL (1972). A reduction in the work function, for instance, allows a larger part of the low-energy electron spectrum to overcome the surface barrier; as this change of the discrimination level acts on the steep slope of the internal energy distribution, the effect on the yield is large. Moreover, the escape depth increases when lower energies are accepted for emission. Consequently, the energy distribution is strongly enhanced at the low-energy end, the peak at the most probable energy is more pronounced, the half-

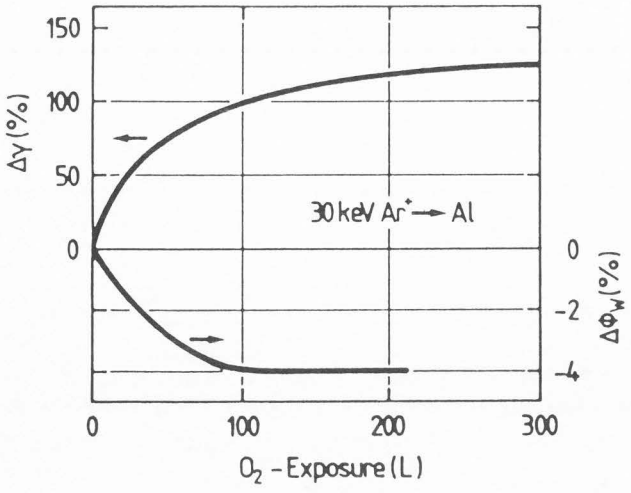

Fig. 4.1: Change of the electron yield and the work function of aluminum upon oxygen exposure. Note that $\Delta\gamma/\gamma$ is very much larger than $|\Delta\Phi_w/\Phi_w|$. The authors, FERRON et al. (1982), ascribe this to emission from an oxide layer.

width decreases.

- electron emission by the adsorbed adatoms themselves, PAETOW and WALCHER (1938). This process could be of influence when the electronic levels of the projectile and adsorbate atom match, leading to an enhanced excitation cross section; it could have led to the apparently target-independent phase in the early measurements of the $\gamma(Z_p)$-dependence. Up to the work of THUM and HOFER (1984), all investigations of the $\gamma(Z_p)$-dependence were carried out on gas-covered surfaces. Such data have great practical importance for quantitative ion detection but are misleading for inferences regarding the physical mechanisms, see Chap. 4.4.

The classical experimental technique for investigating the influence of the work function on electron emission is to deposit on clean metal surfaces alkali or earth alkali atoms in sub-monolayer quantities. Unfortunately, only few such investigations were carried out in the field of kinetic electron emission by ions[6]. In the transition regime of potential to kinetic emission, COGGIOLA (1986) reported for inert gas ions incident on cesiated Mo surfaces that the "change in γ with Φ_w is essentially linear", which is interpreted here as $\Delta\gamma \propto -\Delta\Phi_w$. Owing to the limited range of data this is not necessarily in conflict with the inverse proportionality expressed in Eq.2.7.

The situation is more complex with reactive gases, owing to their frequent incorporation in the bulk. From the unpublished work of FERGUSON (1987) we conclude that adsorption of oxygen and nitrogen on metals such as Au, Ag, and Cu has a much smaller effect on the yield than is commonly associated with these gases from exposure-to-air observations. FERGUSON (1987) found only small yield changes which are, in general, in good correlation with the work-function changes. These changes are, naturally, weak for inert metals. But also for targets of higher chemical affinity like Ti and Pd, the yield changes were small as long as the surface alone is altered. The order-of-magnitude effects, well-known in the literature and evident, for instance, in Figures 4.1 and 4.7, are observed only when the whole excitation regime is affected.

It is to be concluded, therefore, that the pronounced yield increases reported for reactive-gas exposure are due to gas atoms chemically bound in the solid. They cause an increase of the escape depth owing to a reduction in the number of free electrons as energy-dissipative scattering centers.

The work of HASSELKAMP et al. (1980) on oxygen on W, and of FERRON et al. (1982) on oxidation of Al and Mo points in the same direction. While $\Delta\Phi_w$ and $\Delta\gamma$ correlate well in the case of oxygen on Mo and W, the yield increase found for Al (Fig.4.1) is far too large to be explained by a reduction of the work function alone. Rather, it is to be assumed that chemisorbed oxygen diffuses into the Al lattice and transforms the metal surface into an insulating Al_2O_3 layer. Such layers are known to have much larger escape depths for electrons, and thus electron yields.

The same effect occurs on titanium, Fig.4.2. Here the situation is even more complex since oxidation increases both the electron yield and the

[6]Having recourse to the mechanisms obtained in electron-induced electron emission seems to be reliable as long as the Φ_w-influence alone is concerned. This no longer holds true, however, when excitation of the impurities gains in importance.

[7]It might be interesting to note that FERGUSON (1987) could not reproduce the strong yield changes reported by THUM (1979) for air exposure, see e.g. Fig. 2.7, - neither in defined O_2-, N_2-, and H_2-exposures nor in air exposures (all at room-temperature). Air exposures are naturally poorly reproducible, but as these experiments were carried out in the same instrument (but in different laboratories), it appears that gas take-up is promoted by minute components such as H_2O, H_2S, CO, etc. in multi-component gas exposures.

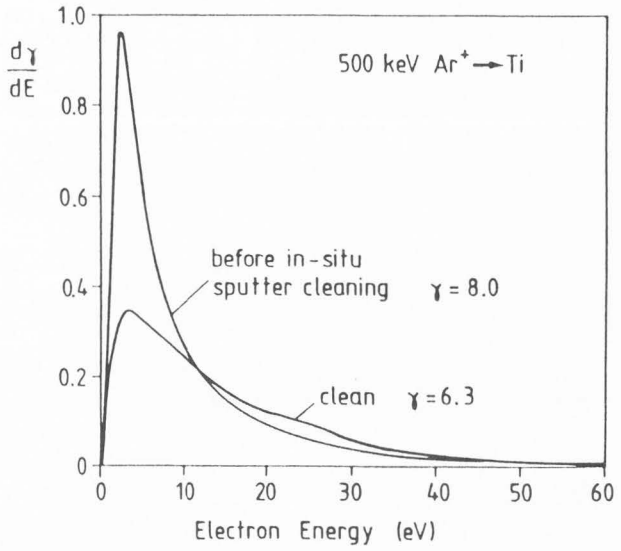

Fig. 4.2: Energy distribution of electrons emitted from air-exposed and sputter-cleaned titanium, respectively. From HASSELKAMP's review (1985).

work function. One should note that there exists a problem in explaning the increase in the low-energy part of the energy spectrum since the assumption of a reduction of the surface barrier clearly does not hold in this case. SCHOU (1980, 1988) pointed out that the binding of free electrons introduces an energy *threshold* below which energetic internal electrons cannot lose energy by exciting bound electrons; the stopping power for these low-energy electrons decreases and this low $dE/dx)^e_{elec}$ - cf.Eq. 2.8 - causes the enhancement in the *low-energy* part of the emitted electron spectrum.

It therefore appears that both the reduction of the surface barrier height and the binding of free electrons act in a similar way on the integral and the energy-differential yields. Consequently, high electron yields are always high partial low-energy yields.

Eventually, we should like to express here again our scepticism about the pertinence of a planar surface barrier for targets without free electrons. A modification of the shape of the barrier towards a spherically symmetric barrier would result in a similar enhancement of low-energy electrons.

4.2 The Dependence of the Yield on the Projectile's Energy

The dependence of the electron yield on the energy or velocity of the projectile has been discussed at various places of this overview: in connection with the separation of potential from kinetic emission (Fig. 2.2), with the correlation between the electron and atom emission yields and the respective electronic and nuclear stopping powers (Fig.2.4), and together with thermionic emission, the emission by cluster ion impact and the influence of surface contaminants (Fig.2.7). Thus, the energy/velocity dependence of the yield appears to be well covered and we limit ourselves here to commenting specific problems in $\gamma(E_p)$ or $\gamma(v_p)$ investigations.

There is firstly the question as to the physically pertinent variable. For obvious practical reasons, the projectile ***energy*** is often chosen in plots and data presentations. Whether or not this is also the physically relevant parameter depends on the prevalent excitation mechanism. In single free-electron excitation as well as in thermal excitation we see no argument against a $\gamma(E_p)$ presentation. Under bombardment conditions where potential or collective excitation are dominant, i.e. where the projectile's interaction time controls the process, the ***velocity*** is the variable to be chosen. In general, the problem stems from the fact that it is seldom one mechanism alone which causes electron excitation. With heavy ion bombardment the case is particularly controversial - apart from the dilemma that instrumental restrictions or constraints of the method often leave no alternative, see e.g. FEHN (1976), THUM and HOFER (1984). Assuming - with the present author - excitation of bound electrons *via* electron promotion in projectile/target-atom collisions to be the leading mechanism for heavy projectiles, one would prefer the velocity as the independent variable.

Electron promotion is, however, not the generally accepted excitation process. ALONSO et al. (1980), for instance, compared - for the case of 2p-hole generation in Al; see for the mechanism Fig. 2.9, and for the data Fig.2.2 - the emission of Auger electrons with that of the integral kinetic electron yield. They found different energy dependencies and took this as an argument against inner-shell excitation. We cannot share this conclusion. The energy dependence of the Auger excitation cross section must deviate from that of γ, even if the whole generation of internal electrons were due to the identical 2p-hole creation process: λ and λ_e are different for these two phenomena (cf. Chap. 2.2.3), and the cascade multiplication process, while being virtually non-existent in Auger electron emission, increases strongly with energy for the integral electron yield. Also, that the ratio of the Auger yield to the electron yield follows different energy dependencies for different projectile ions is

no counter-argument to electron promotion as the leading excitation process in heavy-ion induced electron emission. This is because the projectile ion can be excited as well; excitation functions deviate quite significantly for different orbitals. ALONSO et al. (1980) suggested to consider instead an electron promotion mechanism for *free* electrons; we found this suggestion too diffuse to discuss it here in more detail[8].

What emerges clearly from the investigations of the Bariloche group (BARAGIOLA et al., 1979a; ALONSO et al., 1980) on the energy dependence of electron emission, is a confirmation of BETHE's prediction (cf. Eqs.2.7, 2.8) of a proportionality between γ and $dE/dx)_{elec}$. Such a linear relation was found for hydrogen ions of energy larger than about 20 keV. Excitation of electrons by direct projectile/free-electron collisions was concluded to be the main source term for internal electron generation.

From the work of the Giessen-group (HASSELKAMP et al., 1980-1988) on an even larger variery of projectile/target combinations it is known that this proportionality holds up into the MeV energy regime. Here, there is no more just one excitation mechanism operative but excitation of bound electrons as well as plasmon generation/decay compete with single free-electron excitation. As all these processes contribute to electronic stopping, the γ *versus* $dE/dx)_{elec}$ proportionality is still fulfilled. This is not quite as well the case for He ion bombardment as the data of both studies also show. Moreover, the disagreement with Eqs. 2.7 and 2.8 increases with the projectile mass.

At the other end of the mass scale, i.e. for heavy projectiles such as Kr^+ and Xe^+, the excitation of electrons by energetic recoils gains in importance. Here, the *nuclear* stopping power comes into play for ion-induced electron emission. HOLMEN et al. (1979) state that recoil-induced electron emission "is of crucial importance" for the energy dependence of the yield; in the case of 50 keV incidence of these ions on Cu, for example, they find the electronic energy deposited by recoils to amount about 50 % of that deposited by the projectiles, cf. Eq.2.6. Unfortunately, it is not clear by which excitation mechanism this should happen, if it is by direct projectile/free-electron interaction, the process would be a sub-threshold collision for electron emission. In their work on electron emission from Al and Mo, the Bariloche group (ALONSO et al. (1980), FERRON et al. (1981a, b)) went as far as claiming the whole threshold regime to be "dominated" by recoil effects for these heavy projectiles (especially Kr^+, $Xe^+ \rightarrow$ Al). Their conclusions are based on comparative Monte Carlo computer simulations.

[8]It would, however, be interesting to look more carefully into the possibilities of electron excitation caused by *projectile* de-/excitation when high-velocity ions ($v_p \geq 10^8$cm/s) interact with the electron gas.

4.3 The Dependence of the Yield on the Projectile's Angle of Incidence

There exists a pronounced influence of the angle of projectile incidence on the electron yield. This effect is the origin of the *topography contrast* used in the imaging of surfaces by ion beams - much along the same principle as with secondary electrons in SEMs. Crucial to the topography contrast is the slope of the γ versus ϑ_p-dependence. The physical mechanisms influencing this $\gamma(\vartheta_p)$-dependence will be discussed in the following.

According to Eq. 2.4, the electron yield is directly related to the amount of electronic excitation generated by the projectile within the escape depth λ_e of the target. By varying the incident angle, this amount of excitation energy varies either via the path length of the projectile within λ_e, or by channeling of a fraction of the projectiles across the escape depth. The channeling influence is obviously applicable only to single crystal targets, while path-length variations are effective for both crystalline and amorphous solids.

a. Path-length variations in the escape depth. In the regime of kinetic emission from metals, the electron escape depth is small compared to the projectile range. Thus, by changing the incidence from perpendicular to oblique angles, the path length of the projectile within λ_e is prolonged and thereby its deposition of excitation energy increased. In a simple geometric model, which assumes constant electronic stopping along the track in λ_e and which disregards scattering of the projectiles, a relation of the form

$$\gamma(\vartheta_p) = \gamma(0) \cdot \cos^{-1}\vartheta_p \qquad (4.1a)$$

is expected. $\gamma(0)$ is the yield at perpendicular incidence. For *electron* bombardment it was MÜLLER (1937) who experimentally found Eq.4.1a to hold in the regime of incident angles of $\vartheta_i < 80°$. He also gave the correct quantitative interpretation as well as indicated its limitation. ALLEN (1939) confirmed Eq.4.1a for *proton* bombardment in the 100 keV regime and promoted the model. It has been

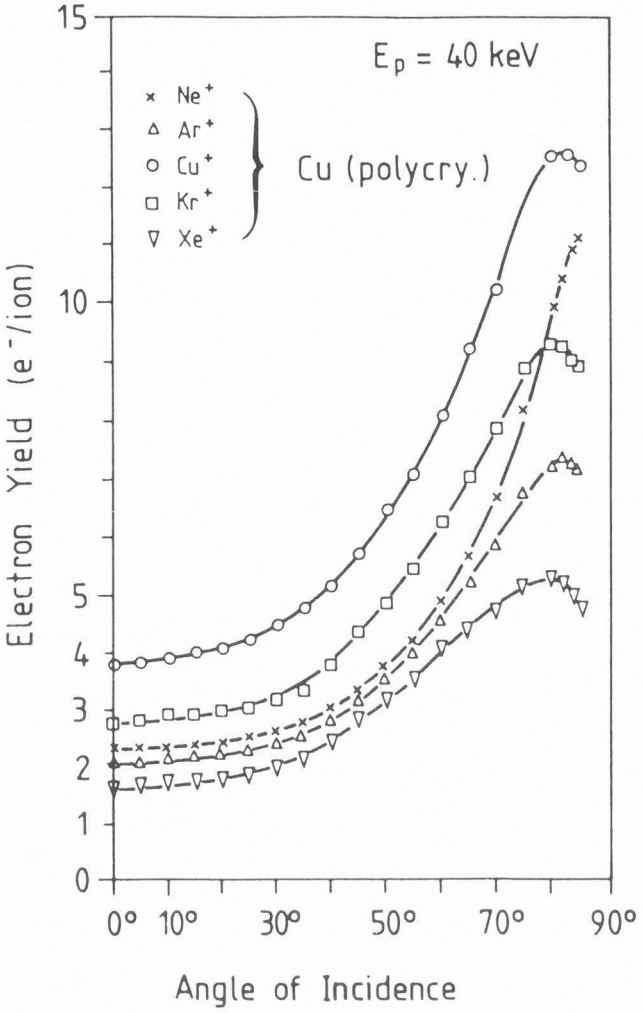

Fig. 4.3: The dependence of the electron yield on the angle of incidence for various projectile ions at a fixed energy. For light ions, represented here by Ne^+, and in the incidence-angle range of $0° < \vartheta_p < 70°$ the yield conforms to a $1/\cos\vartheta_p$ dependence. Deviations from this relation increase with mass, causing the empirical fitting parameter f of Eq. 4.1b to increase from 1.1 for Ne^+ to 1.5 for Kr^+. The authors, SVENSSON et al. (1981), ascribe this to electron excitation by fast recoils. At grazing incidence, $\vartheta_p > 70°$, an increasing portion of the beam suffers scattering from the target surface, resulting in a yield maximum at about 85° followed by a sharp drop.

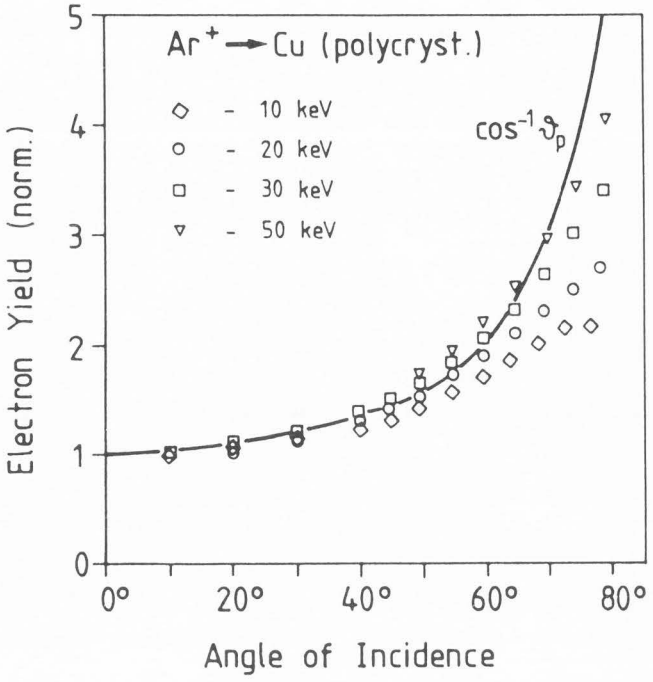

Fig. 4.4: The dependence of the electron yield on the angle of incidence of Ar^+ ions at different energies. With increasing energy the f-parameter of Eq. 4.1b rises from 0.83 to 1.16. The authors, FERRON et al.(1981b), stress the importance of slowing down of the projectile, i.e. not to neglect the reduction of the stopping power while the projectile passes through that region near the target's surface which contributes to electron emission.

confirmed ever since for ***light ions*** above about 1 keV.

For ***heavy ions*** deviations from the simple cosine law exist, as is apparent in Figures 4.3 and 4.4. As with the same phenomenon in the emission of atoms, these deviations are described in a general way by

$$\gamma(\vartheta_p) = \gamma(0) \cdot \cos^{-f}\vartheta_p \qquad (4.1b)$$

where f is a fitting parameter in the range of $0.5 < f < 1.5$. It has no direct physical meaning.

Several reasons can be identified for the deviating from unity of the parameter f

- i- the energy loss of the projectiles during the passage of λ_e cannot be neglected; electron excitation then is no longer proportional to the path length in λ_e; tendency: $f<1$;

-ii- scattering of the projectiles in λ_e causes the assumption of straight-line trajectories to break down; tendency: uncertain, depends on balance of path-length increase by scattering and particle loss by backscattering;

-iii- fast recoils generated in the collision cascade may also excite internal electrons with non-zero ejection probability; tendency: $f>1$;

-iv- the momentum distribution function of

internal electrons is asymmetric in space, its maximum being forward-directed; tendency: $f>1$; Despite recent extended investigations, the incident-angle effect still is controversial in both experiment and theory. In the energy regime considered in this overview, the decreasing efficiency of electronic excitation owing to slowing down of the projectile (process #i) is presumably the dominant one of the above-mentioned mechanisms. Part of this deficiency can be compensated for by the excitation by fast recoils (process #iii), but this requires projectiles heavy in mass and with energies at the upper end of the energy regime considered in this work. Note that the majority of recoils has velocities below the threshold velocity for electron emission of $v_p \approx 5 \times 10^6$ cm/s.

For practical purposes, the deviations from $f=1$ are hardly of importance. If ions are to be used in imaging, preference will always be given to the light ions owing to their lower sputtering yield. Only when sputtering is the effect aimed at - e.g., in surface analysis, repair of microstructures, controlled removal of surface layers, etc. - is imaging by heavy ions worth of consideration.

So far, the glancing-angle regime of $\vartheta_p > 70°$ has been omitted. This regime is difficult to study experimentally owing to beam deflection by the electric field between target and electron collector. Very few reliable measurements exist here, but there is obviously a maximum in the yield near 85°, see Fig.4.3. For quite some time it was not seen at all, cf. ALLEN (1939), MASHKOVA and MOLCHANOV (1963-1965), ZSCHEILE (1965).

Owing to the complications by electric fields, it was rather the analogy to the emission of atoms than studies of electron emission which helped to identify the processes responsible for electron emission at grazing incidence. These processes are violent collisions which scatter the projectiles out of the surface again, to the effect of reducing the energy deposited in the solid - and thus the electron yield as well. When the angle of incidence is increased so far that the projectiles approach the surface at only a few degrees, a collective scattering sets in which prevents the ions from entering the solid at all.In such a surface-channeling mode of ion motion, the projectile skims along ordered surface structures, prohibited from small-impact-parameter, nuclear collisions but still electronically interacting with the solid. Thus there is electron, but no more atom emission. Consequently, the maximum in the $\gamma(\vartheta_p)$-dependence is shifted towards larger incidence angles compared to the $Y(\vartheta_p)$-dependence: in sputtering with heavy ions, the maximum yield is typically reached at $\vartheta_p \approx 70°$ while for electron emission it is observed not below $\vartheta_p \approx 85°$. Comparative studies of this kind led MASHKOVA et al.(1964) to the conclusion that excitation by fast recoils plays no major role in electron emission by grazing-incidence ion bombardment.

b. Reduction of excitation by channeling. Swift particles entering crystalline matter in low-index lattice directions are steered into the interior ($> \lambda_e$) of the target by a multitude of small-angle-scattering collisions. They move in these channels without close-encounter interactions with individual atoms, experiencing only electronic energy loss. This causes a drastic reduction of the *atom* emission yield whenever the projectile-beam direction coincides with a close-packed lattice axis or plane[9]. The sputtering yield decreases because a fraction of the projectiles is steered into regions so deep in the crystal that no more momentum from these projectiles arrives at the surface. Only direct hits, i.e. small-impact-parameter collisions with surface atoms, result in atom ejection events.

Interestingly, *electron* emission also shows this non-monotonous yield versus incidence-angle dependence, Fig.4.5. At first sight this result might appear surprising since electron emission is determined by the deposited electronic energy; this form of energy does not vary as much as the nuclear energy-deposition does when the beam incidence changes from a random to a channeling direction. Certainly not when only free-electron-gas interactions are considered; the electron yield variations shown in Fig.4.5 are too strong to be explained by projectile/free-electron interaction - the prime electronic stopping process in the velocity range below 10^8cm/s. Rather, the effect of projectile channeling on the electron yield is a strong hint that the electronic excitation entailed in small-impact-parameter collisions with target *atoms* are the lead-

[9]Sputtering yield versus incidence-angle measurements provided the first experimental hint of the channeling effect. The relevance of this work of ROL et al. (1959) and MOLCHANOV et al. (1961) to the channeling phenomenon - the matter is briefly reviewed in the articles by ROBINSON and ROOSENDAAL in the monography of sputtering edited by BEHRISCH (1981) - went unnoticed for some years. The non-monotonicity in the *electron*-yield dependence was interpreted right from the start by a lattice transparency model developed by ODINTZOV primarily for interpreting atom emission from single crystals.

ing interaction events in heavy-ion-induced electron emission.

ZSCHEILE's (1965) results, Fig.4.5, also demonstrate that non-monotonicity becomes more pronounced with the mass of the projectile. For the light He^+ ion, the yield minima in the main channeling directions [110], [100], and [112] are barely recognizable, the $\gamma(\vartheta_p)$-dependence resembles more the $1/\cos\vartheta_p$ dependence known from polycrystals; similar results were reported by VON GEMMINGEN (1982) for 5 keV atomic and molecular hydrogen ions incident on Ni (110) and (111) crystal surfaces. Such dependencies, poor in information on the crystal lattice, are characteristic of light (low-Z) projectiles:

According to the theory of channeling, the width of the minima depends on the atomic number and the energy of the projectile as

$$\text{width} \propto (Z_p/E)^{1/4} \qquad (4.2)$$

while the non-channeled fraction in the minimum, i.e. the

$$\text{minimum intensity} \propto (Z_p/E)^{1/2}. \qquad (4.3)$$

Thus, light projectiles have smaller critical channeling angles, the minima are narrower than for heavy projectiles; for this reason, small beam divergence and exact crystal orientation and incidence-angle scanning are critical instrumental preconditions for light ion bombardment. Their neglect result in a smearing-out of the characteristic structures in the $\gamma(\vartheta_p)$-dependence.

In sputtering, numerous studies prove the relevance of Eqs.4.2 and 4.3. The author is not aware, however, of quantitative checks of these dependencies in electron emission. DRENTJE (1967) finds good agreement with (4.2) for the energy dependence of the minima-width for 20 - 80 keV Ar^+ projectiles.

The other reason for the smoother $\gamma(\vartheta_p)$ curves for light projectiles is the larger fraction of free-electron excitation. This interaction is devoid of lattice symmetry. One should be aware, however, of the possibility of ***excitation by backscattered projectiles***. This process is anisotropic owing to the orientation dependence of the backscattering coefficient - which is another consequence of the channeling effect. For instance, about 25 % of 5 keV protons are backscattered from a randomly oriented Ni crystal, while for incidence along a <110> direction the backscattered flux drops to less than 1 % (so-called "aligned geometry" in backscattering

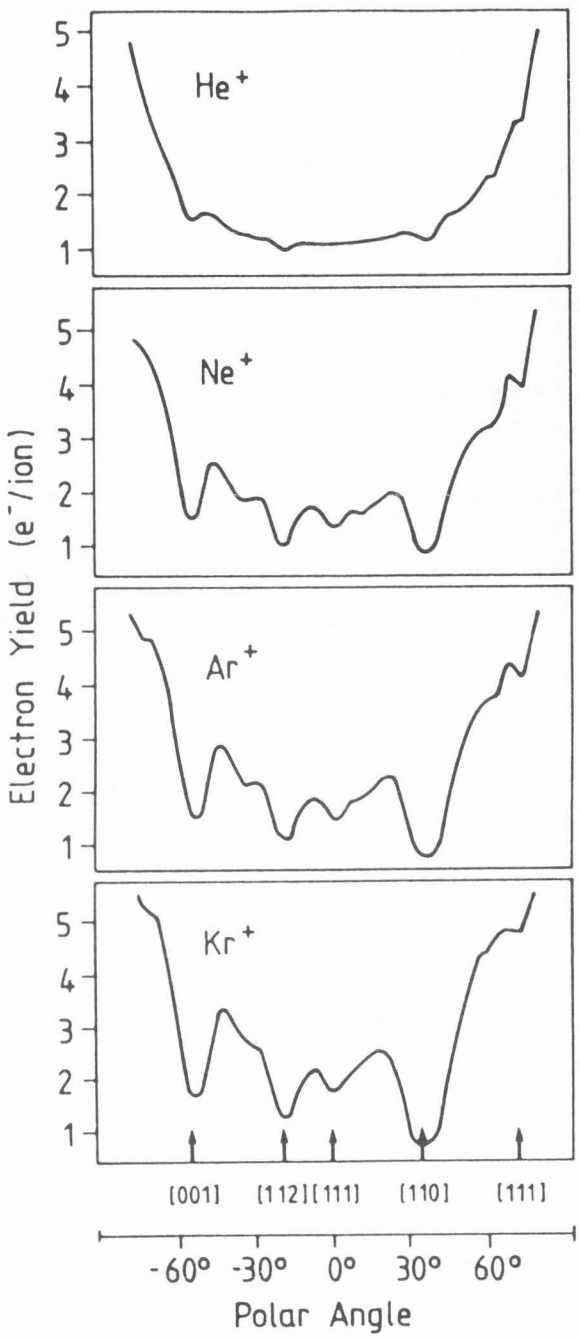

Fig. 4.5: The dependence of the electron yield on the angle of incidence for 26 keV inert gas ions bombarding a Cu (111) single crystal. The crystal was tilted around a [110] axis, perpendicular to the ion beam. Yield minima are observed whenever the ion-beam direction coincides with a close-packed lattice direction. In qualitative accord with the theory of channeling, the width of the maxima increases with projectile mass. From ZSCHEILE (1965).

spectroscopy). We would propose here that it is primarily this effect - free-electron excitation by the orientation-dependent backscattered flux - that causes the non-monotonous $\gamma(\vartheta_p)$ dependence.

It is interesting to interpret in this context the comparative electron, atom, and photon yield measurements of MASHKOVA et al.(1985). For 30 keV Ar^+ ions bombarding (110) and (100) Cu surfaces they find - as in their earlier investigations - the lattice symmetry to be most pronounced in the sputtering yield dependence. Photons characteristic of the Cu atoms, on the other hand, displayed the least lattice influence in their incidence-angle dependence. This is understandable in view of the fact that photon excitation requires the smallest energy transfer (here about 4 eV) in the ion/atom collisions pertinent here. Thus the largest impact parameters apply to photons, leaving the least lattice influence. - With respect to the reduced effect of fast recoils to electron excitation mentioned in the previous chapter, we note that also in this fairly recent work of MASHKOVA et al. the sputtering maximum is reached at incident angles 5° to 10° smaller than for electron emission.

In summary, the dependence of the electron yield on the angle of incidence follows roughly a $1/\cos \vartheta_p$ -dependence up to grazing incidence. For monocrystals, minima are superposed on this dependency which become the more pronounced the higher the mass of the projectile. This non-monotonicity is caused for light projectiles by free-electron excitation by the backscattered flux, and, for heavy projectiles, by the reduction of bound-electron excitation under channeling orientation. At grazing incidence, projectile reflection from the surface causes a sharp drop in the yield to zero.

For further details on the influence of crystal lattice on electron emission the interested reader is referred to:

- the extensive review on (primary **bulk**-) directional effects by BRUSILOVSKY (1985);
- the recent work of PFANDZELTER and coworkers (1988-1990) on electron emission under **surface** channeling conditions;
- the calculations of KITOV and PARILIS (1981, 1984) to the measurements of Toulouse-group on the orientation of **Auger-electron** emission.

4.4 The Dependence of the Yield on the Projectile's Electronic Shell Structure

The electron yield shows a pronounced dependence on the atomic number of the projectile. PLOCH (1950,1951) was not only the first to report this effect, he also gave the correct interpretation,

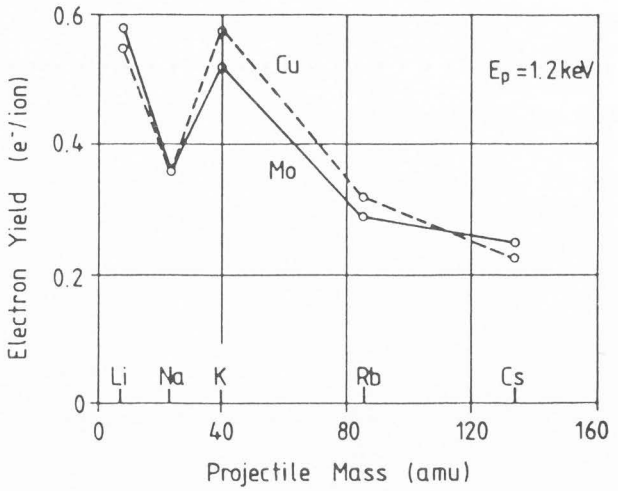

Fig. 4.6: Dependence of the electron yield on alkai-ion bombardment of Cu and Mo surfaces; the targets were de-gassed but, owing to the moderate vacuum conditions, gas-covered during the actual experiment. These data from PLOCH (1950) provided the first indication of an influence of the projectile's electronic shell on electron emission. Note the non-monotonicity even within the same group of the periodic table.

namely the excitation of bound electrons in projectile/target-atom collisions (cf. Chap.2.2.2e). These early results are shown in Fig.4.6. For about 25 years the physics of this effect was overshadowed, however, by its serious implications for ion-detection with the aid of electron multipliers (cf. Chap.3.4). Such detectors were used routinely in mass spectrometers applied for chemical analysis and their varying response to different ions of the periodic table was a matter of considerable concern, VAN GORKOM and GLICK (1970), LAO et al. (1972), POTTIE et al. (1973), FEHN (1976). These measurements provided a data base covering atomic numbers from He to Pb, $2 < Z_p < 80$, which allowed FEHN (1976) to establish the first $\gamma(Z_p)$-plot representative of a large part of the periodic table. In spite of the uncertainties caused by extrapolation and normalization of data of different experimental origin, the γ versus Z_p dependence clearly showed periodic variations superposed on the general velocity dependence of the yield. While the velocity dependence was found to be in good agreement with the PARILISKISHINEVSKII (1960) theory, the undulations were ascribed to electronic shell effects of electronic stopping.

In the same year, STAUDENMAIER et al. (1976) and ROGASCHEWSKI and DÜSTERHÖFT (1976) presented the first results obtained with ion-

electron converters; RUDAT and MORRISON (1978) followed two years later. These data provided absolute electron yields, covered a wider field of projectiles - including molecules and clusters -, and are more reliable as they were obtained by the same experimental setup. Again, a correlation between electronic stopping and $\gamma(Z_p)$ was tentatively inferred and, furthermore, it became clear that molecular projectiles also induce oscillations in the yield.

All these measurements were carried out on gas-covered surfaces. They showed clear oscillations of the yield with the position of the projectile in the periodic table, with little influence of the element of the electron-emitting surface. FEHN (1976) noted, for instance, that a change of the target from CuBe to Al to Ni only reduced in this order the amplitude of the oscillation, the phase remained unaltered; more specifically, in a constant velocity plot of $\gamma(Z_p)$ he found the inert-gas ions always in the maxima, while earth-alkali ions gave minimum yields. These results certainly proved the predominant influence of excitation by the projectile, a closer inspection of the data, however, led to controversies with the excitation model:

In atom/atom collisions, the excitation cross section depends on the electronic structure of both the projectile and the target; it reaches maxima whenever the electronic levels to be excited match. Such a mechanism cannot lead to target-independent phases of the oscillation. Either the (Weizel-Beeck-Fano-Lichten) mechanism does not apply here or the influence of surface contaminants smears out the oscillations specific to the target element. This latter supposition proved indeed to be true as the work of THUM and HOFER (1984) has shown. The yield data in this investigation were obtained with an IEC, in-situ-coated and operated under UHV conditions. In short, it was found that

- the $\gamma(Z_p)$-oscillations for emission from clean Au surfaces are far more pronounced, see Fig.4.7; they are also richer in detail, revealing characteristics of the projectile's electronic shell;

- maxima and minima are not correlated with certain groups in the periodic table, rather they are associated with electronic level matching - which is in perfect agreement with the above-mentioned excitation model (but disagrees with POTTIE et al. (1973) and FEHN (1976));

- contamination of the surface by air strongly changes the $\gamma(Z_p)$ plot in that the data in the minima become much more enhanced than the maxima.

THUM's investigations were continued by FERGUSON (1987) on a variety of clean metal surfaces, mainly in order to investigate the dependence

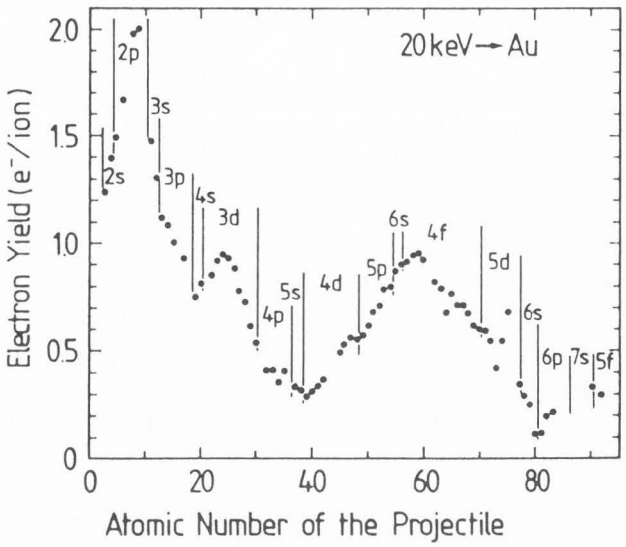

Fig. 4.7: Dependence of the electron yield on the atomic number of the projectile. An in-situ deposited, clean gold surface was bombarded with 20 keV singly charged ions covering 75 % of the elements of the periodic table; the IEC technique was applied to measure the emission statistics, from which the average electron yield can be calculated. As the plot refers to constant energy, the yields decrease with increasing mass. Superposed on this falling tendency are oscillations, the peak-to-peak values of which are at least a factor of 2 larger than on multicomponent surfaces. Cluster and molecule ions also follow this oscillating tendency of the yield. From THUM and HOFER (1984).

on the electronic structure of the target, to check the influence of adsorbed gases (Chap. 4.1), and to look for correlations with electronic stopping. The results relevant to the $\gamma(Z_p)$-oscillations are (FERGUSON and HOFER, 1989):

- the phase of the oscillations ***is*** dependent on the target element, see Fig.4.8, and there are strong hints that the maxima correlate with electronic matching conditions of the colliding atoms;

- the electronic structure of the conduction band has no apparent influence on the oscillations;

- the dependence of the electronic stopping power, when extrapolated down to the comparatively low projectile energies used here, shows no correlation with the $\gamma(Z_p)$-dependence. The reason is given in Chap.2.2.2.

Thus, in summary, the oscillating yield dependence fully supports the notion that the excitation of bound electrons in collisions of multi-electron projectiles with target atoms is the main excita-

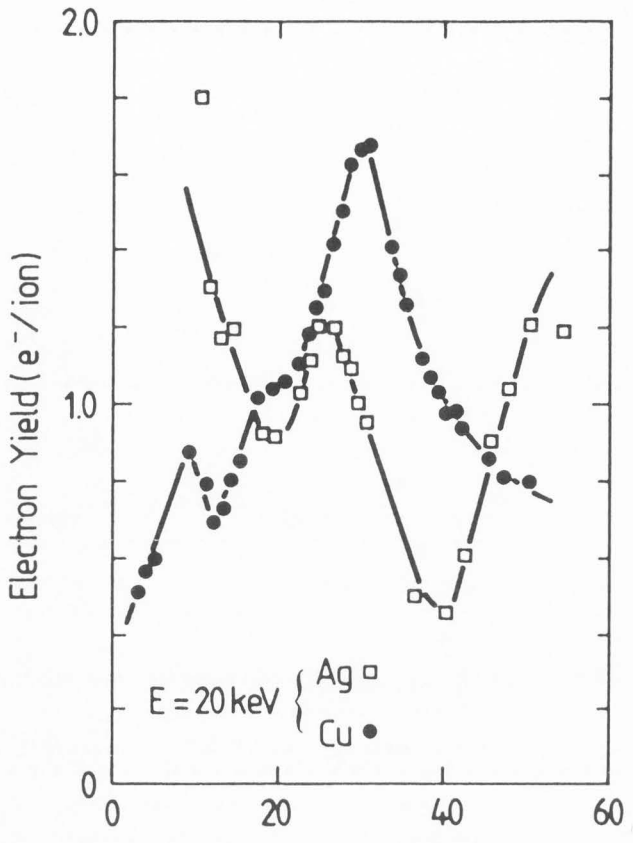

Fig. 4.8: Dependence of the electron yield on the atomic number of the projectile. Silver and copper surfaces were bombarded with 20 keV singly charged ions. In spite of the same work function of Cu and Ag (4.5 eV for (110)-surfaces, for instance) and very similar DOS distribution functions, the $\gamma(Z_p)$-dependency differs markedly for these two metals. From FERGUSON and HOFER (1989).

tion mechanism in the energy regime considered here. In order to understand the fine structure in the $\gamma(Z_p)$-dependence, it is probably necessary to take also projectile excitation into account. The influence of surface contaminants is more intricate than just the effect of an adsorbed surface layer.

4.5 The Angular Distribution

In the regime of kinetic electron emission from amorphous or polycrystalline targets, all investigations agree in that

- the angular distribution is rotationally symmetric around the surface normal,
- this azimuthal symmetry is independent of the angle of projectile incidence ($\vartheta_p \leq 60°$);
- the poloidal distribution follows very closely a cosine law

$$\frac{d\gamma}{d\Omega}(\vartheta) = \frac{d\gamma}{d\Omega}(0) \cdot \cos\vartheta \qquad (4.4)$$

where $d\gamma/d\Omega(\vartheta)$ is the differential yield at the polar angle ϑ. ABBOT and BERRY (1959) studied with rotatable collectors the emission of electrons from tungsten by 40 to 825 eV He^+ ions. All registered distributions conform to a cos ϑ-law, despite the fact that at the low-energy end of projectile incidence, electron emission is due to potential emission. For potential emission, one would intuitively expect a distribution more peaked in the direction of the surface normal ("over-cosine" characteristic). Early calculations by COBAS and LAMB (1944) support this view. Indeed, the work of KLEIN (1965) showed that in potential emission the poloidal angular distribution is more of a $\cos^2\vartheta$ - shape. KLEIN's measurements were carried out on the same target element (W) and with the same technique, but under vacuum conditions better by four orders of magnitude (10^{-9} mbar). For 300 - 4000 eV He^+, Ne^+, and Ar^+ ion incidence, "exact" cosine distributions were observed in kinetic emission, and pronounced forward-peaked distributions in that projectile-velocity regime where the yield was found to be velocity-independent; here, potential emission is prevalent. Moreover, it was observed that these distributions change to a cosine form when the surfaces become gas-covered (i.e. ABBOT & BERRY conditions). Reactive gas layers on W-surfaces increase the work function and, thus, reduce potential emission, cf. Eq. 2.1 and Chap. 4.1. The cos ϑ - distributions found with these targets are then due to the residual kinetic emission.

MISCHLER et al. (1986) found in their investigation of energy-resolved angular distributions from Al bombarded with 25 - 40 keV heavy inert-gas ions, that both the integral electron yield and the Al $L_{23}VV$ Auger electron yield follow closely a cosine distribution.

The physical origin of a cos ϑ- distribution of emitted electrons is an isotropic flux distribution of electrons inside the solid.

The matter is discussed in a slightly confusing way in the literature. Firstly one should note that Eq. 4.4 is not related to the refraction effect on a planar surface barrier (cf. Chap. 2.2.4) as is incorrectly implied in some communications, see e.g., ABBOT and BERRY (1959). A spherically symmetric barrier, for which Eq. 2.25 is replaced by $\vartheta = \vartheta_{in}$ and which, therefore, imposes no refraction on the electrons' trajectories, yields just as well a cosine-shaped emission characteristic. Equation 4.4

expresses simply the flux dependence through a plane tilted by an angle ϑ to the particles' velocity. For the same geometrical reason, the solid angle subtended by the emitting surface decreases with increasing polar-angle position of the detector/collector. On the other hand, the radiation *density* from such surfaces, i.e. the number of particles per unit area and solid angle, is independent of the polar angle. In photometry, emitters of this kind are referred to as Lambert emitters or "isotropically" emitting areas (note that the term is not sensible with point sources). It is perhaps for this reason that the term was used in a double sense with this phenomenon. In particle emission by collision cascades, "isotropic" refers to the internal flux or momentum distribution.

The analogy to photometry can be carried further. ABBOT and BERRY (1959), for instance, correctly point out that "the configuration of an emitting surface may produce a false angular distribution when gross measurements are made, by virtue of the existence on the surface of individual emitting sites with different orientations." This applies directly to structural inhomogeneities, of which beam-induced surface structures (cf. Chap. 3.3) are the most notorious ones in fundamental research on ion-induced electron emission. The authors stress the importance of carrying out the angular scans over a polar-angle range wide enough in order to obtain a true representation of the fundamental emission distribution. The problem is exactly the same in sputtering; LITTMARK and HOFER (1978) developed the theory in this field of particle ejection and gave several demonstrations of angular distributions falsified by faceted surfaces. If not recognized as such, incorrect emission distributions may have serious implications on the understanding of cascade and, more generally, the transport process in the solid.

An isotropic momentum distribution of cascade electrons in the solid is either an indication of spatially symmetric excitation processes, or that the collisions in the electron cascade are efficient enough to average-out anisotropic source distributions. Most of the angular distributions published so far were carried out in an energy regime where excitation of bound electrons by the projectiles is assumed to be the main primary excitation mechanism. This process is presumably spherically symmetric, so spatially isotropic cascades and, eventually, cosine-shaped emission characteristics are not too surprising. In contrast to excitation of bound electrons, excitation of free electrons by projectile/electron collisions is anisotropic. It is not yet clear whether the transport to the surface results in an isotropic cascade distribution and, thus, a cosine emission distribution. We are not aware of any angular distribution measurements obtained under H^+ ion bombardment below about 50 keV; here, this excitation mechanism would be present in its purest form, free of plasmon and bound-electron excitation. The perfectly cosine-shaped profiles obtained with 1 keV He^+ ions (KLEIN, 1965), however, can be taken as an indication of randomization of anisotropic source distributions by electron cascades.

Also Auger electrons appear to follow a cosine-distribution. MISCHLER et al. (1986) found Eq.4.4 to hold for Al $L_{23}VV$ electrons emitted from polycrystalline Al surfaces. The energy of these electrons is 65 eV, resulting in a mean free path length in the target of about 1 nm. Most of the Al LVV electrons originate, therefore, from the top two atomic layers. Also, no randomizing collision cascades can be involved with Auger electrons - as with none of electrons "characteristic" of specific interaction mechanisms (e.g., non-radiative decay, plasmon decay; cf. Chap. 2.2.3)). It is, therefore, the emission process from excited atoms in the solid which must be assumed to be isotropic.

HACHENBERG and BRAUER (1959) showed in their theory of secondary electron emission that in the limit of very low emitted-electron energies, a distribution of the form of Eq. 4.4 is to be expected. By inserting Eq. 2.29a in 2.31 and assuming azimuthal symmetry for the internal distribution function near the surface, i.e.

$$N(0,E_{in},\Omega_{in}) = N(0,E_{in},\vartheta_{in}),$$

one gets the energy-resolved emission distribution in its normalized form

$$\frac{j(E,\vartheta)}{j(E,0)} = \frac{N(0,E_{in},\vartheta_{in})}{N(0,E_{in},0)} \cdot \cos\vartheta \qquad (4.5)$$

which becomes in the limit $E \to 0$, i.e. $E_{in} \to E_{sb}$

$$\to \cos\vartheta \,. \qquad (4.6)$$

This result is, as the authors point out, quite independent of the actual form of $N(x,E_{in},\Omega_{in})$ - apart from its assumed axial symmetry around the surface normal; this assumption becomes questionable at grazing angles of incidence, i.e. at $\vartheta_p > 60°$.

Two more observations by the Toulouse group (MISCHLER et al.,1986, review MISCHLER and BENAZETH, 1986) are interesting to note in this context. Both pertain to Auger electrons and were made on Al targets bombarded under the conditions mentioned before:

Firstly, there is, in addition to the Al LVV electrons, an LMM radiation of distinctly narrower line shape. Such **atom-like Auger electrons** have been reported by several other researchers too (see e.g., WITTMAACK 1979, WHALEY and THOMAS 1984, and the references in THOMAS' review of 1984). For this radiation, MISCHLER et al.(1986) found a polar-angle independent emission distribution, i.e. $d\gamma/d\Omega(\vartheta)$ = const. Such an isotropically radiating source supports the notion that atom-like Auger electrons are due to sputtered excited atoms decaying non-(quantum)radiatively in front of the surface. This deexcitation process takes about 10^{-14} s and is, thus, fast compared to the lifetime determined by radiative decay (typically10^{-8} s). Hence, emission of Auger electrons from sputtered atoms takes place while the ejected atom still is in the vicinity of the surface, whereas photon emission extends some hundreds of nanometers away from the solid. - We note in passing that atom-like Auger electrons are much more intense with heavy-ion bombardment owing to the high sputtering yield of these ions. It is barely visible with light ions and does not exist at all for electron bombardment.

Secondly, there is a weak ($\leq$ 10 %) **azimuthal periodicity** in energy-resolved azimuthal angular distributions from single crystals. By contrast, emission from structureless targets is constant in azimuthal scans at constant polar angle. This periodicity observed with single crystals is correlated with the lattice structure and is more pronounced for the LVV than for the LMM radiation. Owing to the smallness of the effect, we abstain here from an interpretation but should like to remark that a full understanding of the anisotropic emission of LMM radiation requires to take into account the anisotropic emission of *atoms* in single-crystal sputtering; in sputtering, the intensity modulation in constant-polar-angle scans is of the order of 100 % and, thus, very much more pronounced than in electron emission (see e.g. ROBINSON's and HOFER's reviews in the BEHRISCH's monographs on sputtering, Vol.1 and 3 of 1981 and 1991, respectively).

4.6 The Energy Distribution

The energy distribution of electrons emitted from metal surfaces is a typical cascade distribution, modified by the refraction effect at the transition of the electrons from the solid to the vacuum. The gross features of electron spectra are, therefore, not so much determined by the primary excitation but by the development of the electron cascade. FÜCHTBAUER's (1906b) observation of a relative independence of the energy distribution of the projectile's energy (4 - 21 keV), mass (N^+, H^+,e^-), and angle of incidence is understandable from this point of view.

Less understandable is his high most probable energy of $\hat{E} \approx 30$ eV. The peak in the energy spectrum is typically a few electron volts and thus an order of magnitude smaller than found in the early measurements. One should note, however, that these studies were carried out with hydrogen ions; with these light projectiles, the energy transfer is more effective which could shift the spectrum towards higher energies. SCHNEIDER (1931), who performed the first energy distribution measurements in *transmission* (20 - 50 keV $H^+ \rightarrow$ Au) and, thereby, identified the maximum energy transfer to free electrons (Eq. 2.14) from the spectrum's cut-off energy, also found shifted energy spectra. HILL et al.'s (1939) statement concerning the energy of electrons emitted from Mo, Pb, Al, and Cu by 40 - 400 keV hydrogen ions lies in a similar vein. We are not aware of precision measurements of the energy distribution of electrons emitted in the *backward* direction by protons below 50 keV; such spectra could provide valuable insight into the contribution of backscattered projectiles to electron emission; we would expect them to be to be slightly "harder" than spectra obtained with heavy ions. An $\hat{E}$ as high as 30 eV is, however, probably an error in the measurement.

Representative electron spectra obtained under heavy ion bombardment are shown in Figs. 4.2 and 4.9. It is apparent in Fig. 4.9 that the main effect of projectile-parameter changes is an increase of fast electrons whenever the energy transfer increases. The most probable energy, on the other hand, is little influenced. On the grounds of emission from an electron cascade initiated by a fast internal electron - generated either by ionization or by direct projectile/electron collisions - the shape of the energy distribution can be quantatively described:

Arguments can be put forward for an isotropic internal flux distribution of the form

$$j_{in} \propto E_{in}^{-2} \qquad (4.7a)$$

in the electron energy interval of $1 < E_{in} < 100$ eV, see SCHOU (1980, 1988). With the transformation relation for ejection through a plane surface barrier, Eq. 2.31, this yields

$$\frac{d\gamma}{dE} \propto \frac{E}{(E+E_{sb})^3}\cos\theta \qquad (4.8a)$$

Differentiation with respect to E gives the most

probable energy

$$\hat{E} = E_{sb} / 2 \qquad (4.9)$$

Equations 4.8a and 4.9 are in rough qualitative agreement with experiment. They reproduce well the functional dependency's insensitivity of the projectile parameters. This is, apparently, particularly well fulfilled in the emitted-energy interval around the most probable energy.

A more general analytical expression for the internal flux was deduced by SCHOU (1980). He finds

$$j_{in} \propto 1 / [\, E_{in} \cdot dE/dx)^{e}_{elec} \,] \qquad (4.7b)$$

which gives with Eq. 2.31 the energy spectrum of emitted electrons as

$$\frac{dy}{dE} \propto \frac{E}{(E+E_{sb})^2 \frac{dE}{dx}\Big]^{e}_{elec}} \qquad (4.8b)$$

For the electronic stopping power for internal electrons of energy $E_{in} < 30$ eV he proposes to use

$$dE/dx)^{e}_{elec} \propto E_{in}^{3}, \qquad (4.10)$$

which gives for the most probable energy values about a factor of 2 lower than Eq. 4.9. In the case of Al, for example, the data read: $E_{sb} = 15.6$ eV, $\hat{E}_{theo} \approx 8$ eV, $\hat{E}_{exp} \approx 2$ eV; there is, thus, still room for further improvement.

We add in passing that the formalism inherent in the derivation of Eqs.4.8 and 4.9 is the same as that in the emission of atoms from surfaces. The development of transport-theoretical treatments of electron emission preceded that for sputtering by about a decade. In the regime of emission of atoms by nuclear collision cascades, the agreement between theory and experiment is good even by quantitative standards. Equation 4.9, for instance, has been used to evaluate the surface binding energy relevant to collisional emission; it is generally felt that the thermodynamic sublimation energy, which is generally used as the surface barrier energy in sputtering, is only a rough approximation to an otherwise inaccessible quantity.

An interesting and equally important observation is that many non-metallic surface layers as well as adsorbed impurities cause a strong increase of the low-energy part of the spectrum, see Fig. 4.2. This effect is well documented in secondary electron emission, see HACHENBERG and BRAUER

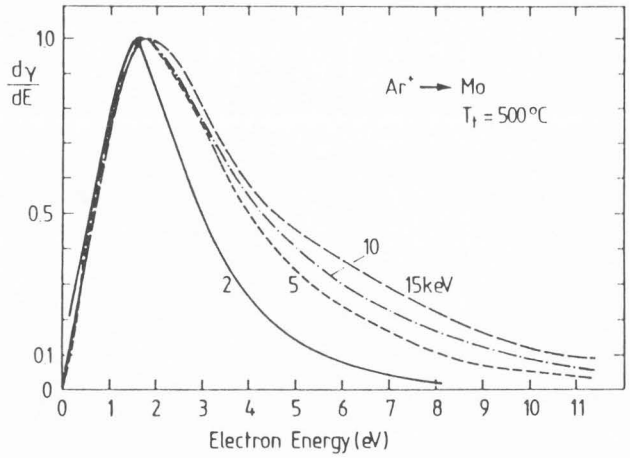

Fig. 4.9: Energy distribution of electrons emitted from a Mo surface upon bombardment with 2, 5, 10, and 15 keV Ar^+ ions. The measurements were carried out in poor vacuum (10^{-6} mbar with mostly inert gases in the residual gas) but some cleaning was achieved by heating the target to 500° C during the measurements; also, the ion bombardment results in removal of surface contaminants. The most probable electron energy is $\hat{E}$ = 1.7 eV for 5 to 15 keV Ar^+, and 1.9 eV for He^+ ions. The results for He^+ bombardment are not shown here, but it is noted that the 5 keV Ar^+ and the 2 keV He^+ spectra practically coincide. From WEHNER (1966).

(1959) and the work of APPELT discussed therein, PALMBERG (1967), SCHAEFER and HOELZL (1972). In fact, it appears that the high yields of composite surfaces are due to this increase of the partial low-energy yield. All these high-yield targets are non-conducting, TAKEISHI (1962), BAUMHÄCKEL (1967a,b). We stress here again the conceptual problematics of assigning a work-function type surface barrier, cf. Chaps. 2.2.4 and 4.1.

Only in the case of surface adsorbates is the change of the energy distribution understood. In Chap. 4.1 we have discussed this effect of the work function in terms of its discriminating action on the internal energy spectrum. In that chapter we have also indicated the interpretational complication with altered surface layers extending into the bulk. In many such cases - of which the oxides, nitrides, and hydrides are most noteworthy - the influence of an increased escape depth by far outweighs the effect of the surface barrier. The surface barrier may in- or decrease upon reactive-gas influence, the electron yield always increases. Apparently (Fig. 4.2), this increase affects predominantly the low-

energy part of the energy spectrum. Whether this is due to a change of the internal distribution function, N_{in}, or a modified surface barrier *shape*, cannot be conclusively answered here.

It is doubtful whether the formal parameter variation in AMELIO's (1970) theory of electron spectra carried out by SCHAEFER and HOELZL (1972) is appropriate for non-conductors. But it might be helpful to summarize their results, in particular since they are in general well reproduced in SCHOU's (1980) theory: A decreasing work function - at constant Fermi energy - results in:

- a decreasing most probable energy $\hat{E}$, (cf. Eq. 4.9);
- an increasing intensity at $\hat{E}$;
- a decreasing half-width of the spectral distribution.

A decreasing Fermi energy - at constant work function - results in:

- a decrease of the most probable energy;
- a decrease of the half-width of the spectral distribution.

This latter assumption means, in essence, a decreasing energy band width of the internal electron reservoir. Applied to non-conductors: the binding of conduction electrons by, for instance, sorption of reactive gases in metals, also results in narrowing the band width of the electron source term. The predictions of SCHAEFER and HOELZL's (1972) calculations are at least qualitatively in keeping with the change of energy spectra from air-exposed to clean Ti shown in Fig. 4.2.

4.7 The Emission Statistics

The emission of electrons from solids is a stochastic process. It is based on a random series of collisions, the impact-parameter distribution of which is random also. When viewed on an atomic scale, there is thus a great variety in the collision sequences and, consequently, a wide spread in the number of emitted electrons from one projectile impact to the other. To be meaningful, the assignment of characteristic quantities, such as the yield, for instance, requires the registration of a great number of emission events. These quantities reveal no information on the particular sequence of collisions following an individual projectile impact.

This is a well known fact, of course, in all emission phenomena from multi-particle systems. In electron emission by ion bombardment the possibility exists, however, to measure the emission statistics, viz. the frequency distribution of emission of $\gamma = 1,2,3,...$ electrons per incident projectile. Such measurements are performed with the help of ion-electron converters. This method was discussed in Chap. 3.4, particularly with regard to the determination of the average yield $\bar{\gamma}$; most investigations sofar aimed at $\bar{\gamma}$. Electron yields are, however, not the most valuable information obtainable with the converter technique: it is the possibility of investigating the emission statistics that renders this technique so attractive. In its ultimate consequence, it would allow the specification of any kind of collision sequence that lead to the emission of a given number γ of electrons per ion; for instance, it would allow to specify those - presumably near-surface collisions - that result in high electron emission ($\gamma = 5$, for example, in Fig. 3.3); and it would give insight in those interaction sequences, where the projectile deposits all its electronic interaction energy in sub-threshold form, hence precluding excited electrons from crossing the solid/vacuum interface ($\gamma = 0$). These zero-emission events are, for example, of eminent importance in quantitative ion detection, where they are responsible for the counting losses. As they are not accessible to a direct measurement, counting losses need to be determined from the emission statistics.

Only a short outline of the present status of knowledge on emission statistics can be given here. This knowledge is rich in uncertainties. There is, firstly, the still not settled question on the nature of the deviations of measured emission distributions from a Poisson statistics: is the larger width of the experimentally determined frequency distribution an instrumental artefact, cf. Chap. 3.4, or is it of a genuine origin? This would call for a probability function different from the one anticipated for a purely random process, viz. the Poisson distribution. Most modern investigations - i.e. those performed with high-resolution solid state detectors - agree in that Poisson distributions do not give entirely satisfactory fits. The fits are good enough for $\bar{\gamma}$ determinations of the above-stated accuracy, but they lack in consistency in order to allow the identification of the appropriate distribution function.

Following the work of PRESCOTT (1966), and DIETZ and SHEFFIELD (1973, 1975) it has become common practice in electron emission to use the Polya distribution function to fit experimental frequency distributions. The Polya distribution is a compound Poisson distribution. It is composed of a Poisson and a Laplace (or Gamma) distribution and has the form

$$P(\gamma;\bar{\gamma},b) = \frac{\bar{\gamma}^{\gamma}}{\gamma!}\,(1+b\bar{\gamma})^{-\gamma-1/b}\cdot\prod_{i=1}^{\gamma}[1+(i-1)b] \qquad (4.11)$$

where the first parameter, $\bar{\gamma}$, is the mean of the distribution, and the second, $0 \leq b \leq 1$, determines its width. The width, as defined by its relative variance, is

$$\text{width} \equiv \frac{\text{variance}}{(\text{mean})^2} = \bar{\gamma}^{-1} + b\,. \qquad (4.12)$$

It is a characteristic feature of compound Poisson distributions that their mean is identical with that of the underlying Poisson disribution, and that the relative variances of the two distribution functions involved are additive. There are two limiting cases: for $b = 0$ the distribution is Poissonian, while in the case of $b = 1$ Eq. 4.11 yields a quasi-exponential decrease of the probability of multi-electron emission with increasing γ; this distribution is referred to as the Furry distribution and has been popular in early stage-gain and pulse-shape calculations in photomultipliers, see e.g., the references in PRESCOTT (1966).

It is trivial that a two-parameter distribution is capable of giving better fits to experimental data than the one-parameter Poisson distribution. Accepting $b > 0$ to be not of an instrumental origin leaves to answer, however, the fundamental question as to the physical meaning of this parameter. What is the physical mechanism that broadens the emission distribution beyond a Poisson distribution? The aforementioned authors offered the following interpretation: the genuine electron emission process could be truly Poissonian, but the "effective" emission may vary from place to place on the emitting surface; this spatial variation may be due to alterations of stoichiometry and/or structure on the surface, or it may be caused by an emission-site dependent collection efficiency for the emitted electrons. Whatever the reason for the variation of the "effective" emission may be, if the variation conforms to Laplace's function the combination of these two probability distributions yields Eq. 4.11. In this interpretation, the convenience of a compound Poisson distribution becomes obvious: the average yield, as determined by fitting Eq. 4.11 to the (unfolded) experimental frequency distribution, remains characteristic of the actual electron emission process, while the parameter b represents the variation of these average yields due to an effect which may or may not be an artefact.

Obviously, the stoichiometry argument for a justification of $b > 0$ does not hold for clean monatomic targets. It was, however, the clean-monatomic-surface case in the work of THUM (1979) which required $b > 0$ for an improved fit to the experimental data. For a multi-component target such as stainless steel, on the other hand, the distributions were found to be almost perfectly Poissonian ($b = 0$) - as did STAUDENMAIER et al., (1976) and DEV (1990), on gas-covered surfaces.

Regarding the spacially variable collection efficiency, the extensive ray-track simulations by HOFER and LITTMARK (1976) showed no indication of a pronounced electron discrimination; FERGUSON (1987) listed further arguments against an instrumental origin for the deviations from a Poisson statistics. Still, for the reasons discussed in Chap 3.4 this possibility cannot entirely be dismissed.

Occasionally negative b values appear in the output of the numeric deconvolution procedure. In these very rare cases - which should, on the grounds of the Polya statistics, actually be discarded - the distribution function is *narrower* than the Poisson distribution. DIETZ and SHEFFIELD (1973, 1975) are of the opinion that this indicates the bias of the basic statistical process in ion-induced electron emission toward a binomial distribution; to this distribution the Poisson statistics is only an approximation, the authors pointed out. We would add that it is, for the time being, a well acceptable approximation in many projectile/target combinations. In order to achieve further refinements, very detailed instumental and numerical efforts will be required.

We should like to conclude by drawing again a parallel to the emission of atoms. There exists as yet no experimental method of measuring the emission statistics in sputtering. With the help of a Monte Carlo simulation code, ECKSTEIN (1988) studied the frequency distributions of multi-atom emission and found Poisson distributions insufficient for a proper description of the simulation results. He, too, used Polya distributions; no explanation on physical grounds could be given so far. In sputtering, multi-atom emission is of particular interest in the field of cluster emission. One should note, however, that these two phenomena are not synonymous. Clusters are *bound* particles, emitted presumably in a collective collision event, see e.g. GNASER and HOFER (1989) or the present authors's review in BEHRISCH's monograph of sputtering. Neither the binding nor the collective criterium apply for multi-atom emission. A deeper insight in the statis-

tics of atom emission is of vital importance for an understanding of sputtering on an atomistic scale, i.e., on the grounds of individual elastic slowing-down and collision cascade events.

5. Summary and Outlook

Our status of understanding of the phenomenon of kinetic emission of electrons from the surface of solids upon ion bombardment is still highly unsatisfying. This applies to both the experiment and theory.

With regard to the experimental situation, electron yields still cannot be extra- or interpolated from reliable data sets. With clean metal surfaces, this uncertainty is primarily a consequence of the pronounced effect of the electronic shell structure of the projectile/target atom combination. Electronic shell effects are partly also responsible for the apparently wide scattering of yields obtained on multi-component targets. The main reason for this scatter is, however, the strong influence of composition changes on the transport of electrons in the solid and on the height of the escape barrier at the surface.

The lack of data for insulators is embarrassing, particularly in view of the great applicational importance of these high-yield emitters. Compared to this deficiency, the scarcity of yield data for metals at projectile energies above the maximum of the electronic stopping power is more of an academic lapse. Such high-energy yields would be helpful for checking theories over a wider energy span and for establishing handy scaling relations.

The full understanding of the phenomenon and the development of a microscopic theory of electron emission is complicated by the multitude of excitation mechanisms in the solid. It is a matter of course, that those experimental results are particularly helpful where one excitation mechanism can be identifyed to be dominating. We anticipate that in this respect integral yields, angular distributions and energy distributions at low-energy (< 50 keV) hydrogen bombardment would promote the understanding of electron emission by excitation in collisions between projectiles and free electrons. With heavy ions in this energy range, on the other hand, the problem lies not so much in data reliable enough to cross-check calculations, but in our poor knowledge of outer-shell excitation in atom/atom collisions; here, investigations on photon and electron emission from gas targets could provide valuable information. However, already the next step in the treatment, the nonradiative decay of the excited atom with the involvement of electrons from the conduction band, requires solid state effects to take into account. This applies even more so to electron transport by collision cascades and the escape of electrons across the surface barrier. Owing to these complications, we do not expect a microscopic theory of ion-induced electron emission to be available on a quantitative basis in the next years to come.

Phenomenological theories, which assume electron emission to be determined by the electronic stopping power of the projectile near the surface, exist in various degrees of sophistication. They all suffer from the fact that for heavy ions in the velocity range considered here ($v_p < v_H \approx 2\times10^8$ cm/s), electronic stopping and electron emission are controlled by different excitation effects. This disparity in the dominant excitation mechanisms - and, as a consequence, the inaccuracy of the results - is alleviated at projectile velocities larger than the orbital velocity of bound electrons. In a strict sense, such theories yield results with acceptable quantitative agreement with experiment only for hydrogen ions (at $v_p \geq 2\times10^8$ cm/s, corresponding to energies $E_p \geq 20$ keV).

The possibility of studying the emission statistics of electrons is a unique opportunity in the whole field of particle-induced emission from solids. By its very nature, electron emission provides information primarily on the electronic part of the interaction process. But, by way of recoil-generated electrons, also some information on elastic interaction - scattering of projectiles in particular - may be extractable from statistics data. Although recognized since more than a decade, emission statistics still awaits the experimental and mathematical-physical exploration. This field, as well as research on insulating surfaces, will see the advantages of ion-electron converters to be used more often than was appreciated in the past.

Acknowledgements

I should like to thank M. M. Ferguson for many fruitful discussions and for allowing reference to still unpublished results of her work. D. Hasselkamp and J. Schou kindly read a rather preliminary manuscript and helped with many stimulating comments. I am also grateful for the hospitality shown me by the staff of the Solid State Division during a sabbatical year at the Oak Ridge National Laboratories.

References

Review Articles on Particle-Induced Electron Emission[10]

Abroyan IA, Eremeev MA, Petrov NN. (1967). Excitation of electrons in solids by relatively slow atomic particles. Sov. Phys. Uspekhi **10**, 332-367.

Arifov U. (1969). *Interaction of Atomic Particles with a Solid Surface.* Consultants Bureau, New York - London.

Baragiola RA. (1982). Principles and Applications of Ion-Induced Auger Electron Emission from Solids. Radiat. Eff. **61**, 47-72.

Benazeth N. (1982). Review of Kinetic Ion-Electron Emission from Solid Metallic Targets. Nucl. Instr. Meth. **194**, 405-413.

Bruining H. (1954). *Physics and Applications of Secondary Electron Emission*, Pergamon Press, London.

Brusilovsky BA. (1985). Directional Effects in Kinetic Ion-Electron Emission. Vacuum **35**, 595-615.

Brusilovsky BA. (1990). Kinetic Ion-Induced Electron Emission from the Surface of Random Solids. Appl. Phys. A**50**, 111-129.

Carter G, Colligon J. (1968). In: *Ion Bombardment of Solids*. Amer. Elsevier Co. Inc., p.38-74.

Hachenberg O, Brauer W. (1959). Secondary Electron Emission from Solids. In: *Advances in Electronics and Electron Physics*. Vol. 11, 413-499. Academic Press, New York.

Hasselkamp D. (1985). *Die ionen-induzierte kinetische Elektronenemission von Metallen bei mittleren und großen Ionenenergien*. Habilitationsschrift Universität Gießen, Germany.

Hasselkamp D. (1988). Secondary Emission of Electrons by Ion Impact on Surfaces. Comments At. Mol. Phys. **21**, 241-255.

Hennequin JF, Viaris de Lesegno P. (1980). Ion-Induced Auger Electron Emission from Solids. In: *The Physics of Ionised Gases*, SPIG'80,Ed.: M. Matic, B. Kidric Inst. Nucl. Sci., p. 341-378.

Hofer WO. (1980). Emission of Atoms and Electrons from High-Density Collision Cascades in Metals. Nucl. Instr. Meth. **170**, 275-279.

Hofer WO. (1987). Plasma-Surface Interactions: The role of charged particle emission. J. Vac. Sci. Technol. A**5**, 2213-2216.

Kaminsky M. (1965). *Atomic and Ionic Impact Phenomena on Metal Surfaces*, Academic Press.

Krebs KH. (1968). Electron Ejection from Solids by Atomic Particles with Kinetic Energy. Fortschr. d. Physik **16**, 419-490.

Krebs KH. (1983). Recent Advances in the Field of Ion-Induced Kinetic Electron Emission from Solids. Vacuum **33**, 555-563.

Lai SY, Briggs D, Brown A, Vickerman JC. (1986). The Relationship between Electron and Ion Induced Secondary Electron Imaging: A review with new experimental observations. Surface and Interface Analysis **8**, 93-111.

Landolt M. (1985). *Spin Polarized Secondary Electron Emission from Ferromagnets*, in R. Feder (Ed.): *Polarized Electrons in Surface Physics*. World Scientific Publ. Co., Singapore.

Levi-Setti R. (1983). Secondary electron and ion imaging in scanning ion microscopy. Scanning Electron Microsc. **1983**;I, 1-22.

Massey HS, Burhop EHS. (1951). In: *Electronic and Ionic Impact Phenomena*. Oxford Press, p. 542-557.

Medved DB, Strausser YE. (1965). Kinetic Ejection of Electrons from Solids. Adv. Electr. Electron Phys. **21**, 101-179.

Mischler J, Benazeth N. (1986). Ion-Induced Auger Emission from Solid Targets. Scanning Electron Microsc. **1986**;II, 351-368.

Parilis ES. (1968). Kinetic Electron Emission and Fast Ion Bombardment. IAEA Vienna: A Survey of Phenomena in Ionized Gases, 309-349.

Schou J. (1988). Secondary Electron Emission from Solids by Electron and Proton Bombardment. Scanning Microsc. **2**(2), 607-632.

Seiler H. (1982). Secondary Electron Emission. Scanning Electron Microsc. **1982**;I, 33-42.

Sigmund P, Tougaard S. (1981). Electron Emission from Solids during Ion Bombardment: Theoretical Aspects. Springer Ser. in Chemical Physics **17**, 2-37.

Thomas EW. (1984a). Secondary Electron Emission. Nucl. Fusion, Spec. Issue, Ed.: RA Langley et al., 94-104.

Thomas EW. (1984b). Ion bombardment induced photon and Auger emission for surface analysis. Vacuum **34**, 1031-1044.

Varga P. (1987). Neutralization of Multiply Charged Ions at a Surface. Appl. Phys. **A44**, 31-41.

Review Articles on Related Subjects[11]

Beeck O. (1934). Über den Durchgang langsamer positiver Ionen durch hochverdünnte Gase. Physikal. Zeitschr. **35**, 36-52.

Behrisch R.(Ed., Vol.3 with K. Wittmaack):

[10], [11]References referring to review articles are addressed as such in the text.

Sputtering by Particle Bombardment:

Vol.1: *Physical Sputtering of Single-Element Solids* (1981);

Vol.2: *Sputtering of Alloys and Compounds, Electron and Neutron Sputtering, Surface Topography* (1983);

Vol.3: *Distribution of Sputtered Particles, Applications* (1990);

in Springer series *Topics in Applied Physics*, Springer-Verlag, Berlin.

Ertl G, Küppers J. (1985). *Low Energy Electrons and Surface Chemistry*, VCH Verlagsgesellschaft, Weinheim, Germany.

Garcia JD, Fortner RJ, Kavanagh TM. (1973). Inner-Shell Vacancy Production in Ion-Atom Collisions. Rev. Mod. Phys. **45**, 111-177.

Gemmel DS. (1974). Channeling and related effects in the motion of charged particles through crystals. Rev Mod. Phys. **46**, 129-227.

Joyes P. (1973). Theoretical models in secondary ionic emission. Radiat. Effects **19**, 235-241.

Kiriakidis G, Carter G, Whitton JL. (1986). *Erosion and Growth of Solids Stimulated by Atom and Ion Beams*. M. Nijhoff Publ., Boston.

Levi-Setti R, Wang YL, Crow G. (1986). Scanning ion microscopy: Elemental maps at high lateral resolution. Appl. Surf. Sci. **26**, 249-264.

Lichten W. (1980). Molecular Orbital Model of Atomic Collisions. J. Phys. Chem. **84**, 2102-2116.

Massey HSW, Burhop EHS, Gilbody HB. (1974). *Electronic and Ionic Impact Phenomena*, Vol. IV *Recombination and Fast Collisions of Heavy Particles*, Clarendon Press, Oxford, U.K.

Raether H. (1980). *Excitation of Plasmons and Interband Transitions by Electrons*, Springer Verlag, Berlin.

Sigmund P. (1975). Energy loss of charged particles in solids. In *Radiation Damage Processes in Materials*.Ed.: CHS Dupuy, Noordhoff, Leyden, The Netherlands, p. 3-117.

Stolterfoht N. (1987). High resolution Auger spectroscopy in energetic ion atom collisions. Physics Reports **146**, 315-424.

Wittmaack K. (1977). Secondary ion production due to ion-surface bombardment. Proc. Int. Worksh. *Inelastic Ion-Surface Collisions*, Eds.: N. Tolk et al., Academic Press, New York, p.153-199.

Ziegler JF. (1980). *Handbook on stopping cross sections for energetic ions in all elements.* Pergamon Press, New York.

Ziegler JF, Biersack JP, Littmark U. (1985). *The stopping and range of ions in solids*. Pergamon Press, New York.

Original Contributions

Abbott RC, Berry HW. (1959). Measurement of the Angular Distribution of Electrons Ejected from Tungsten by Helium Ions. J. Appl. Phys. **30**, 871-873.

Allen JS. (1939). The Emission of Secondary Electrons from Metals Bombarded with Protons. Phys. Rev. **55**, 473-478.

Alonso EV, Alurralde MA, Baragiola RA. (1986). Kinetic Electron Emission from Solids Induced by Slow Heavy Ions. Surface Sci. **166**, L155-L160.

Alonso EV, Baragiola RA, Ferron J, Jakas MM, Oliva-Florio A. (1980). Z_1 dependence of ion-induced electron emission from aluminum. Phys. Rev. B **22**, 80-87.

Amelio GF. (1970). Theory for the Energy Distribution of Secondary Electrons. J. Vac. Sci. Technol. **7**, 593-604.

Asselt WK van, Poelsema B, Boers AL. (1978). Electron back-scattering in a surface-barrier detector. J. Phys. D: Appl. Phys., **11**, L 107-110.

Austin L, Starke H. (1902). Ueber die Reflexion der Kathodenstrahlen und eine damit verbundene neue Erscheinung sekundärer Emission. Annalen d. Physik (Leipzg.) **9**, 271-282.

Baklitsky BE, Parilis ES. (1972). The Role of Electron Shells in Kinetic Electron Emission and Luminescence under Ion Bombardment. Radiat. Eff. **12**, 137-138.

Baklitsky BE, Parilis ES. (1986). Inelastic energy loss and electron emission resulting from ion bombardment of a solid surface. Sov. Phys. Tech. Phys. **31**, 15-19.

Banouni M, Mischler J, Negre M, Benazeth N. (1985). Surface topography effects on energy resolved polar angular distributions of ion-induced secondary electrons. Surface Sci. **163**, L720-L729.

Baragiola RA, Alonso EV, Ferron J, Oliva-Florio A. (1979a). Ion-induced Electron Emission from Clean Metals. Surface Sci. **90**, 240-255.

Baragiola RA, Alonso EV, Oliva-Florio A. (1979b). Electron emission from clean metal surfaces induced by low-energy light ions. Phys. Rev. B**19**, 121-129.

Baragiola R, Ferron J, Zampieri G. (1984). Effect of Oxygen on Secondary Ion Emission from Aluminium. Nucl. Instrum. Meth. Phys. Res. B**2**, 614-616.

Barrington RE, Anderson JM. (1958). The Probability of Multiple Emissions of Secondary Electrons. Proc. Roy. Soc. **72**(5), 717-726.

Barut AO. (1954). The Mechanism of Second-

ary Electron Emission. Phys. Rev. **93**, 981-984.

Baumhäkel R. (1967a). Elektronenemission von intermetallischen Verbindungen bei Ionenbeschuß. Untersuchung von aktiviertem und unaktiviertem CuBe. Z. Physik **199**, 41-55.

Baumhäkel R. (1967b). Untersuchung von Casium-Antimon-Schichten. ibid. 56-67.

Becker A. (1924). Über die durch α-Strahlen erregte Elektronenemission. Annalen d. Physik **75**, 217-275.

Becker A. (1925). Über die Geschwindigkeit der sekundären Kathodenstrahlung. ibid. **78**, 228-252.

Benazeth C, Benazeth N, Viel L. (1978). Spectres Auger et sections efficaces d'ionisation de la couche L_{23} du magnesium et de l'aluminium sous impact de protons et d'ions lourdes (10-100 keV). Surface Sci. **78**, 625-647.

Bethe HA. (1941). On the theory of secondary emission. Phys. Rev. **59**, 940.

Beuhler RJ. (1983). A comparison of secondary electron yields from accelerated water cluster ions ($M/z < 50000$) striking Al_2O_3 and Cu surfaces. J. Appl. Phys. **54**, 4118-4126.

Beuhler RJ, Friedman L. (1977a). Low Noise, High Voltage Secondary Emission Ion Detector for Polyatomic Ions. Int. J. Mass Spectrom. Ion Phys. **23**, 81-97.

Beuhler RJ, Friedman L. (1977b). A model of secondary electron yields from atomic and polyatomic ion impacts on copper and tungsten surfaces based upon stopping-power calculations. J. Appl. Phys. **48**, 3928-3936.

Beuhler RJ, Friedman L. (1980). Threshold studies of secondary electron emission induced by macro-ion impact on solid surfaces. Nucl. Instr. Meth. **170**, 309-315.

Bindi R, Lanteri H, Rostaing P. (1987). Secondary electron emission by reflection induced by electron bombardment of polycrystalline metallic targets. Scanning Microscopy **1**(4), 1475-1490.

Blauth EW, Draeger WM, Kirschner J, Liebl H, Müller N, Taglauer E. (1971). Experimental and Statistical Investigations on the Measurement of Very Low Ion Currents in Mass Spectrometers. J. Vac. Sci.Technol. **8**, 384-387.

Boerboom AJH, Schram BL, Kleine W, Kistemaker J. (1966). Einfluß der Geschwindigkeit von Edelgasionen auf die Emission von Sekundär-Elektronen. Z. Naturforschg. **21a**, 127-129.

Brunnée C. (1957). Über die Ionenreflexion und Sekundärelektronenemission beim Auftreffen von Alkaliionen auf reine Molybdän-Oberflächen. Z. Physik **147**, 161-183.

Brusilovskii BA, Molchanov VA. (1978). Ion-electron Emission from a Spherical Target. Sov. Tech. Phys. Lett. **4**, 383-387.

Budzioch J, Soszka M, Soszka W. (1986). Effect of violent collisions in ion-electron emission. Nucl. Instr. Meth. Phys. Res. B**14**, 530-534.

Cafolla AA, Carter JN, Delaney CFG, McDonald IR. (1975). A computation on secondary electron emission statistics and its application to single electron spectra in photo- and electron multipliers. Nucl. Instr. Meth. **128**, 157-161.

Cailler M, Barzine K, Roptin D, Ganachaud JP. (1985). A Monte-Carlo calculation of elastic and inelastic escape functions for Auger electrons emitted from aluminium. Surface Sci. **154**, 575-600.

Campbell N. (1915). Ionization by Positive Rays. Phil. Mag. **23**, 783-794.

Carlston CE, Magnuson GD, Mahadevan P, Harrison Jr. DE. (1965). Electron Ejection from Single Crystals due to 1 to 10-keV Noble-Gas Ion Bombardment. Phys. Rev. **139**, A729-A736.

Cawthorn ER. (1971). Secondary Electron Emission from Solid Surfaces Bombarded by Medium Energy Ions. Aust. J. Phys. **24**, 859-869.

Cheney WL. (1917). The Emission of Electrons by a Metal when Bombarded by Positive Ions in a Vacuum. Phys. Rev. **10**, 335-347.

Cobas A, Lamb WE. (1944). On the Extraction of Electrons from a Metal Surface by Ions and Metastable Atoms. Phys. Rev. **65**, 327-337.

Coggiola MJ. (1986). Secondary Electron Yields from Mo and Mo/Cs Surfaces by Ion Impact. Nucl. Instr. Meth. B**13**, 641-644.

Cook N, Burtt RB. (1975). 1-17 keV Positive-ion-induced Electron Ejection from Tungsten, Molybdenum and Vanadium. J. Phys. D: Appl. Phys. **8**, 800-811.

Daly NR. (1960). Scintillation type Mass Spectrometer Ion Detector. Rev. Sci. Instr. **31**, 264-266.

Delaunay M, Geller R, Debernardi J, Ludwig P, Sortais P. (1988). Electron emission from a metal surface bombarded by highly charged ions. Surf. Sci. **197**, L273-L280.

Dev B. (1982). Detection of low energy ion-induced secondary electron emission; dependence on the angle of incidence. Appl. Surface Sci. **10**, 240-246.

Dev B. (1990). Statistics of secondary electrons from W induced by He ions and atoms at 0° - 90° incidence. Appl. Surface Sci. **40**, 319-326.

Dietz LA, Sheffield JC. (1973). Spectrometer for Measuring Secondary Electron Yields Induced by Ion Impacts on Thin Film Oxide Surfaces. Rev.

Sci.Instr. **44**, 183-191.

Dietz LA, Sheffield JC. (1975). Secondary electron emission induced by 5-30 keV monatomic ions striking thin oxide films. J. Appl. Phys. **46**, 4361-4670.

Drentje SA. (1967). Remarks on the kinetic ejection of electrons from a copper monocrystal by argon ions with energy 20-80 keV. Phys. Lett. **24**A, 12-14.

Dubus A, Devooght J, Dehaes JC. (1986). A Theoretical Evaluation of Ion Induced Secondary Electron Emission. Nucl. Instrum. Methods Phys. Res. B**13**, 623-626.

Dubus A, Devooght J, Dehaes JC. (1987). Improved age-diffusion model for low-energy electron transport in solids. I. Theory. Phys. Rev. B**36**, 5093-5109.

Dubus A, Devooght J, Dehaes JC. (1987). Improved age-diffusion model for low-energy electron transport in solids. II. Application to secondary electron emission from aluminum. ibid. 5110-5119.

Eckstein W. (1988). Statistics of sputtering. Nucl Instr. Meth. Phys. Res. B**33**, 489-492.

Fagot B, Fert C. (1964). Emission electronique secondaire de monocristaux de cuivre en fonction de l'orientation du faiseau ionique incident. C. R. Acad. Sci. (France) **258**, 1180-1183.

Fagot B, Colombie N, Fert C. (1964). Coefficients d'emission secondaire de cibles monocrystallines de cuivre sous bombardement ionique. ibid. 4670-4673.

Fano U, Lichten W. (1965). Interpretation of Ar^+ - Ar Collisions at 50 keV. Phys. Rev. Lett. **14**, 627-629.

Fehn U. (1974). Isotope Effect of Ion-Electron Emission. Int. J. Mass Spec. Ion Phys. **15**, 391-397.

Fehn U. (1976). Variance of Ion-Electron Coefficients with Atomic Number of Impacting Ions. Int. Mass Spec. Ion Phys. **21**, 1-14.

Ferguson MM. (1987). Ioneninduzierte kinetische Elektronenemission an reinen und gasbedeckten Metalloberflächen. Thesis Techn. Universität Wien, Austria. Also published as report Jül-2201 (1988), ISSN 0366-0885.

Ferguson MM, Hofer WO. (1989). On the Z_1 Dependence of Ion-induced Kinetic Electron Emission. Radiat. Eff. Def. Solids. **109**, 273-280.

Fehringer M, Delaunay M, Geller R, Varga P, Winter H. (1987). Potential Emission for Multi charged ion Impact on Clean Tungsten above the Kinetic Emission Threshold. Nucl Instr. Meth. B**23**, 245-247. See also Phys. Rev. B**35**, 4232-4235.

Ferron J, Alonso EV, Baragiola RA, Oliva-Florio A. (1981a). Electron Emission from Molybdenum under Ion Bombardment. J. Phys. D **14**, 1707-1720.

Ferrón J, Alonso EV, Baragiola RA, Oliva-Florio A. (1981b). Dependence of Ion-Electron Emission from Clean Metals on the Incidence Angle of the Projectile. Phys. Rev. B**24**, 4412-4419.

Ferrón J, Alonso EV, Baragiola RA, Oliva-Florio A. (1982). Ion-Electron Emission: The Effect of Oxidation. Surf. Sci. **120**, 427-434.

Füchtbauer Ch. (1906a). Über eine von Kanalstrahlen erzeugte Sekundärstrahlung und über eine Reflexion der Kanalstrahlen. Physikal.Zeitschr. 7Jg. Nov. 5, p. 153-157.

Füchtbauer Ch. (1906b). Über die Geschwindigkeit des von Kanalstrahlen und von Kathodenstrahlen beim Auftreffen auf Metalle erzeugten Strahlen. ibid.748-750. An extended abstract of this work appeared in Verhandlg. Dt. Physikal. Ges. **8** (1906) 349.

Füchtbauer Ch. (1907). Über Sekundärstrahlung. Ann. d. Physik **23**, 301-307.

Ganachaud JP, Cailler M. (1979). A Monte-Carlo calculation of the secondary electron emission of normal metals. Surface Sci. **83**, 498-518.

Gemmingen U v. (1982). Ion Induced Secondary Electron Emission from Single Crystal Surfaces. Surface Science **120**, 334-346.

Gingerich KA. (1968). The "Mass" Effect of Electron Multipliers in High Temperature Mass Spectrometric Applications. Advances in Chemistry Ser., Vol. 72: *Mass Spectrometry in Inorganic Chemistry,* American Chem. Soc., Washington, p. 291-300.

Gnaser H, Hofer WO. (1989). The Emission of Neutral Clusters in Sputtering. Appl.Phys. A**48**, 261-271.

Gorkom M v., Glick RE. (1970). Electron Multiplier Response under Positive Ion Impact I. Secondary Electron Emission Coefficients. Int. J. Mass Spec. Ion Phys. **4**, 203-218.

Greupner H. (1968). Zur Statistik der atomteilcheninduzierten Elektronenauslösung aus Festkörpern. Z. Physik **214**, 427-436.

Greupner H, Gaworzewski P. (1969). Zum Nachweis der Elektronenmehrfachemission mittels Szintillationszähler. Int. J. Mass Spectrom. Ion Phys. **3**, 365-370.

Grizzi O, Baragiola RA. (1984). Be K-shell Auger-electron emission in slow-ion - surface collisions. Phys. Rev. A**30**, 2297-2303.

Gullikson E. (1988). Hot-electron diffusion lengths in the rare-gas solids. Phys. Rev. B**37**, 7904-7906.

Gurtovoi ME. (1940). Concerning the problem

of the kinetic nature of collisional generation of secondary electrons by positive ions. Zhur. Eksp. i. Teor. Fiz.**10**, 483-496 (in Russian).

Gurtovoi ME. (1941). Emission of secondary electrons from ThW due to impacts of ions and atoms under the conditions of mercury discharge. Zhur. Eksp. i. Teor. Fiz.**11**, 489-502 (in Russian; the paper deals with potential emission).

Häussler P. (1964). Untersuchungen zur Mehrfach-Emission von Sekundärelektronen. Z. Physik **179**, 276-284.

Hagstrum HD. (1954a). Auger Ejection of Electrons from Tungsten by Noble Gas Ions. Phys. Rev. **96**, 325-335.

Hagstrum HD. (1954b). Theory of Auger Ejection of Electrons from Metals by Ions. ibid. 336-365.

Harrison Jr. DE, Carlston CE, Magnuson GD. (1965). Kinetic Emission of Electrons from Monocrystalline Targets. Phys. Rev. **139**, A737-A745.

Hasselkamp D, Scharmann A. (1982). The Ion-Induced Low Energy Electron Spectrum from Aluminum. Surface Sci. **119**, L388-L392.

Hasselkamp D, Hippler S, Scharmann A. (1987). Ion-induced secondary electron spectra from clean metal surfaces. Nucl Instr. Meth. Phys. Res. B**18**, 561-565.

Hasselkamp D, Hippler S, Scharmann A. (1987). Electronic Processes Induced by High Energy H^+, H_2^+, and H_3^+ Ions: A Scaling Relation. Z. Physik D**6**, 269-274.

Hasselkamp D, Lang KG, Scharmann A, Stiller N. (1981). Ion Induced Electron Emission from Metal Surfaces. Nucl. Instrum. Methods **180**, 349-356.

Hasselkamp D, Scharmann A, Stiller N. (1980). Ion Induced Secondary Electron Emission as a Probe for Adsorbed Oxygen on Tungsten. Nucl. Instrum. Methods **168**, 579-583.

Healea M, Chaffee EL. (1936). Secondary Electron Emission from a Hot Nickel Target Due to Bombardment by Hydrogen Ions. Phys. Rev. **49**, 925-930.

Healea M. (1939). Comparison of the Secondary Electron Emission Due to H_2^+ and D_2^+ Ions. Phys. Rev. **55**, 984.

Healea M, Houtermans C. (1940). The Relative Secondary Electron Emission Due to He, Ne, and Ar Ions Bombarding a Hot Nickel Target. Phys. Rev. **58**, 608-610.

Hedin A, Hakansson P, Sundqvist BUR. (1987). On the detection of large organic ions by secondary electron production. Int. J. Mass Spectr. Ion Proc. **75**, 275-285.

Herold D, Schoenheit E. (1965). Ein Ionenwandler-Detektor mit Gate-Schaltung für massenspektrometrische Untersuchungen. Z. angew. Physik **20**, 102-112.

Herold D. (1965). Untersuchung der Sekundärelektronen-Emission von Kupfer-Beryllium durch positive Ionen bei einer Energie von 25 keV. ibid. **113**, 8.

Herrmann M. (1965). Untersuchung verschiedener Elektronenemissionsprozesse auf Mehrfachemission. Z. Physik **184**, 352-354.

Hill AG, Buechner WW, Clark JS, Fisk JB. (1939). The Emission of Secondary Electrons under High Energy Positive Ion Bombardment. Phys. Rev. **55**, 463-470.

Hippler S. (1988). Spezielle Aspekte der Ionen-induzierten Elektronenemission: Eine Untersuchung von Strukturen im niederenergetischen Emissionsspektrum und zur Z_2-Abhängigkeit des Sekundärelektronenemissionskoeffizienten. Thesis Universität Giessen, Germany.

Hippler S, Hasselkamp D, Scharmann A. (1988). The ion-induced electron yield as a function of the target material. Nucl. Instr. Meth. Phys. Res. B**34**, 518-520.

Hird B, Pepin C, Kelly G. (1984). Charge dependence of secondary electron emission coefficients. J. Appl. Phys. **56**, 3304-3307.

Hofer WO, Littmark U. (1976). Ion and Electron Trajectories in Mirror-Type Ion-Electron Converters. Nucl. Instr. Meth. **138**, 67-75.

Hofer WO, Thum F. (1978). A simple axially-symmetric quadrupole SIMS spectrometer. Nucl. Instr. Meth. **149**, 535-541.

Holmén G, Svensson B, Schou J, Sigmund P. (1979). Direct and Recoil-induced Electron Emission from Ion-bombarded Solids. Phys. Rev. B**20**, 2247-2254.

Holmén G, Svensson B, Burén A. (1981). Ion Induced Electron Emission from Polycrystalline Copper. Nucl. Instr. Meth. **185**, 523-532.

Holst G, Oosterhuis E. (1921). Over de electrische geleiding in gasen. Physica **1**, 78-87.

Holst G, Oosterhuis E. (1923). The Sparking-potential of Gases. Phil. Mag. **46**, 117-122.

Jackson WJ. (1927). Secondary Emission from Mo Due to Bombardment by High Speed Positive Ions of the Alkali Metals. Phys. Rev. **30**, 473-478.

Kapitza P. (1923). On the Theory of δ-Radiation. Phil. Mag. **45**, 989-998.

Kitov VU, Parilis ES. (1981). Orientational Effects in the Ion-Excited Auger Electron Emission. Surface Sci. **107**, 363-375.

Kitov VU, Parilis ES. (1984). The Role of

Recoil Atoms in Ion-Excited Auger Electron Emission from Single Crystals. Surface Sci. **138**, 202-210.

Klein HJ. (1965). Ausbeuten und Winkelverteilungen der durch Edelgasionen an reinen Wolframoberflächen ausgelösten Sekundärelektronen. Z. Physik **188**,78-92.

Kollath R, Simon KH. (1964). Bemerkung zur Mehrfach-Emission von Sekundärelektronen. Z. Physik **179**, 274-275.

Krueger FR. (1977). Zum Mechanismus der Spaltfragment-induzierten Desorption. Z. Naturforsch. **32a**, 1084-1092.

Kuznetsov AA, Protopopov OD. (1979). Electron energy spectra in the excitation of GaAs and InP by argon ions. Sov. Tech. Phys. Lett. **5**(1), 40-41.

Lakits G, Aumayr F, Winter H. (1989a). Statistics of potential electron emission. Radiat. Eff. Def. Sol. **109**, 129-136.

Lakits G, Aumayr F, Winter H. (1989b). Statistics of ion-induced electron emission from a clean metal surface. Rev. Sci. Instr. **60**, 3151-3159.

Lakits G, Aumayr F, Winter H. (1989c). Statistics of electron emission from metal surfaces bombarded by ions in different charge states. J. Physique. C1, Suppl. 1, 533-539.

Lindhard J, Nielsen V, Scharff M. (1968). Approximation Method in Classical Scattering by Screened Coulomb Fields. Mat. Fys. Medd. Dan. Vid. Selsk. **36**, No. 10

Lao RC, Sander R, Pottie RF. (1972). Discrimination in Electron Multipliers for Atomic Ions. 1. Multiplier Yields for 24 Mass-Analyzed Ions. Int. J. Mass Spec. Ion Phys. **10**, 309-313.

Large LN. (1963). The Effect of Absorbed Gases on Proton Induced Electron Emission from Titanium. Proc. Phys. Soc. **81**, 175-180.

Littmark U, Hofer WO. (1978). The influence of surface structures on sputtering: Angular distribution and yield from faceted surfaces. J. Mater. Sci. **13**, 2577-2586.

Mahadevan P, Layton JK, Medved DB. (1963). Secondary Electron Emission from Clean Surface of Molybdenum Due to Low-Energy Noble Gas Ions. Phys. Rev. **129**, 79-83.

Mahadevan P, Magnuson GD, Layton JK, Carlston CE. (1965). Secondary-Electron Emission from Molybdenum Due to Positive and Negative Ions of Atmospheric Gases. Phys. Rev. **140**, A1407-A1412.

Makarov VV, Petrov NN. (1981). Regularities of secondary electron emission of the elements of the periodic table. Sov. Phys. Solid State **23**, 1028-1031.

Mashkova ES, Molchanov VA. (1965). Influence of thermal lattice vibrations on the anisotropy of the secondary electron emission coefficient of single crystals. Sov. Phys.-Sol. State **6**, 2967-2967.

Mashkova ES, Molchanov VA, Fleurov VB. (1985). Angular Dependences of Sputtering Ratio, Ion-Electron Emission Coefficient and Ion-Induced Photon Emission Yield at Oblique Ion Incidence on Crystalline Targets. Radiat. Eff. **89**, 313-318.

Mashkova ES, Molchanov VA, Odintsov DD. (1963). Anisotropy of the ion-electron emission coefficient of single crystals. Doklad. Akad. Nauk SSSR **151**, 1074-1075; engl. transl.: Sov. Phys. Doklad. **8**, (1964) 806-807.

Mashkova ES, Molchanov VA, Odintsov DD. (1964). Anisotropy of the sputtering ratio and of the ion-electron emission coefficient in single crystals. Soviet Phys.- Sol. State **5**, 2516-2518.

Mischler J, Nègre M, Benazeth N. (1982). Energy-Resolved Angular Distributions of Secondary Electrons Emitted from (111) Al Target Bombarded by Different Inert Gas Ions. Surf. Sci. **118**, 193-207.

Mischler J, Banouni M, Benazeth C, Nègre M, Benazeth N. (1986). Surface Topography Effects on Energy-Resolved Polar Angular Distributions of Electrons Induced in Heavy Ion-Al Collisions: Experiments and Models. Radiat. Eff. **97**,1-20.

Mischler J, Benazeth N, Nègre M, Benazeth C. (1984). Angular Distributions of Secondary Electrons Emitted in Ar^+-Polycrystalline Al Collisions. Surf. Sci. **136**, 532-544 and ibid. **163** (1985) L720-L729.

Mischler J, Maurel B, Benazeth N. (1989). The Influence of Cone-covered Surface Structures on Sputtering and Secondary Electron Emission: Model. Radiat. Eff. Def. Solids **108**, 145-157.

Morgulis ND. (1939). On the question of the nature of cathode sputtering and kinetic electron emission. Z. Eksper. Teoret. Fiz. **9**, 1484-1494. (No official English translation available? German translation available from W.O. Hofer).

Morgulis ND. (1941). Concerning the Nature of Cathode Sputtering and Kinetic Emission of Secondary Electrons. Z. Eksp. Teoret. Fiz. **11**/2-3, 300-302 (in Russian).

Müller HO. (1937). Die Abhängigkeit der Sekundärelektronenemission einiger Metalle vom Einfallswinkel des primären Kathodenstrahls. Z.Physik **104**, 475-486.

Negre M, Mischler J, Benazeth N. (1985). Azimuthal angular distributions of Xe^+ and Kr^+ ion-induced Al L_{23} Auger electrons. Surface Sci. **157**,

436-450.

Oechsner H. (1978). Electron yields from clean polycrystalline metal surfaces by noble-gas-ion bombardment at energies around 1 keV. Phys. Rev. B**17**, 1052-1056.

Oliphant MLE. (1930). The Liberation of Electrons from Metal Surfaces by Positive Ions. Part I. Experimental. Proc. Roy. Soc. London A**127**, 373-387.

Oliphant MLE, Moon PB. (1930). The Liberation of Electrons from Metal Surfaces by Positive Ions. Part II. Theoretical. ibid. p. 388-406.

Ortykov A, Rakhimov R. (1988). Ion-Electron Emission of Cs Films on the (110) and (111) Faces to Mo Single Crystals. Radiotekh. Electron. No.2, 363-370. Engl. transl.: Sov. J. Communicat. Technolog. Electronics (USA) **33**/7, 74-80.

Paetow H, Walcher W. (1938). Über den Einfluß von Adsorptionsschichten auf die Auslösung von Elektronen und die Reflexion von Ionen beim Auftreffen von positiven Caesiumionen auf Wolfram. Z. Physik **110**, 69-83.

Palmberg PW. (1967). Secondary Emission Studies on Ge and Na-Covered Ge. J. Appl. Phys. **38**, 2137-2147.

Parilis ES, Kishinevskii LM. (1960). The Theory of Ion-Electron Emission. Sov. Phys. Solid State **3**, 885-891.

Parker Jr. JH. (1954). Electron Ejection by Slow Positive Ions Incident on Flashed and Gas - Covered Metallic Surfaces. Phys. Rev. **93**, 1148-1156.

Pfandzelter R, Schuster M. (1988). Surface Analysis of Crystals by Surface Channeling. Nucl. Instr. Meth. Phys. Res. B**33**, 898-904.

Pfandzelter R. (1989). Oberfächengitterführung an Silizium. Thesis Universität München; see also the thesis of H. Winter (1986) on Ni.

Pfandzelter R. (1990). Auger Electron and Secondary Electron Yields Induced by Surface Channeled Protons. Nucl. Instr. Meth. Phys. Res. B (in press); see also the article with JW Lee in Surface Sci. **225**, 301-306.

Ploch W. (1951). Massenabhängigkeit der Elektronenauslösung durch isotope Ionen. Z. Physik **130**, 174-195. See also the short communication in Z. Naturforschg. **5a** (1950) 570-571.

Pottie RF, Cocke DL, Gingerich KA. (1973). Discrimination in Multipliers for Atomic Ions. II. Comparison of yields for 61 atoms. Int. J. Mass Spec. Ion Phys. **11**, 41-48.

Prescott JR. (1966). A statistical model for photomultiplier single-electron statistics. Nucl Instr. Meth. **39**, 173-179.

Rösler M, Brauer W. (1981a). Theory of Secondary Electron Emission. I. General Theory for Nearly Free-Electron Metals. phys. stat. sol. (b) **104**, 161-175.

Rösler M, Brauer W. (1981 b). Theory of Secondary Electron Emission. II. Application to Aluminum. phys. stat. sol. (b) **104**, 575-587.

Rösler M, Brauer W. (1984). On the Theory of Ion-Induced Electron Emission. phys. stat. sol. (b) **126**, 629-642.

Rösler M, Brauer W. (1988). Theory of Electron Emission from Solids by Proton and Electron Bombardment. phys. stat. sol. (b) **148**, 213-226.

Rösler M, Brauer W. (1989). Influence of Dynamic Screening on the Electron Yield - Stopping Power Relation for Proton Impact in Aluminum. phys. stat. sol. (b) **156**, K 85-87.

Rogaschewski S, Düsterhöft H. (1976). Z_1-Dependence of Kinetic Ion-Electron Emission from a Gas-Covered Stainless-Steel Surface. phys. stat. sol. (b) **75**, K173.

Rudat MA, Morrison GH. (1978). Detector Discrimination in SIMS: Ion-to-Electron Converter Yield Factors for Positive Ions. Int. J. Mass Spectr. Ion Phys. **27**, 249-261.

Rutherford E. (1905). Charge carried by the α and β Rays of Radium. Phil. Mag. **10**, 193-208.

Schackert P. (1966). Zur Sekundärelektronenemission durch Argonionen und Argonatome im Energiebereich von 1 bis 20 keV. Z. Physik **197**, 32-40.

Schaefer J, Hoelzl J. (1972). A contribution to the dependence of secondary electron emission from the work function and Fermi energy. Thin Solid Films **13**, 81-86.

Schneider G. (1931). Auslösung von Sekundärelektronen durch Wasserstoffkanalstrahlen in Metallen. Ann. Physik **11**, 357-384.

Schou J. (1980). Transport theory for kinetic emission of secondary electrons from solids. Phys. Rev. B**22**, 2141-2174.

Schütze W, Bernhard F. (1956). Eine neue Methode zur Messung extrem kleiner Ionenströme im Hochvakuum. Z. Physik **145**, 44-47.

Sigmund P. (1969). Theory of Sputtering. I. Sputtering Yield of Amorphous and Polycrystalline Targets. Phys. Rev. **184**, 383-416.

Simon KH, Herrmann M, Schackert P. (1965). Nachweis der Mehrfachemission von Sekundärelektronen mittels Proportionalzählrohr. Z. Physik **184**, 347-351.

Soszka W. (1990). Ion-Induced Electron Emission from the Cold Metal Targets Covered by Rare Gases. Nucl. Instr. Meth. Phys. Res., in press

Soszka W, Kwasny S, Budzioch J, Soszka M. (1989). Ion-electron emission from a cold metal target covered by xenon. J. Phys.: Condens. Matter **1**, 1353-1363.

Soszka M, Soszka W. (1983). A new observation method of ion-electron emission. Phys. Letters **97**, A 256-258.

Staudenmaier G, Hofer WO, Liebl H. (1976). Cluster Induced Secondary Electron Emission. Int. J. Mass Spectr. Ion Phys. **21**, 103-112.

Stein JD, White FA. (1972). New Method for the Measurement of Electron Yield from Ion Bombardment. J. Appl. Phys. **43**, 2617-2620.

Sternglass EJ. (1957). Theory of Secondary Electron Emission by High-Speed Ions. Phys. Rev. **108**, 1-12.

Streitwolf HW. (1959). Zur Theorie der Sekundärelektronenemission von Metallen. Der Anregungsprozess. Ann. d. Physik. **3**, 183-196.

Svensson B, Holmén G. (1981). Electron Emission from Ion-bombarded Aluminum. J. Appl. Phys. **52**, 6928-6933.

Svensson B, Holmén G, Burén A. (1981). Angular Dependence of the Ion-Induced Secondary-electron Yield from Solids. Phys. Rev. B**24**, 3749-3755.

Svensson B, Holmén G, Linnros J. (1982). Electron Emission from Silver under heavy Atomic and Molecular Ion Bombardment. Nucl. Instr. Meth. **194**, 429-432.

Takeishi Y. (1962). Ejection of Electrons from Barium Oxide by Noble Gas Ions. J. Phys. Soc. Japan, **17**, 326-341.

Thomson JJ. (1904). On the positive electrification of α rays, and the emission of slowly moving cathode rays by radio-active substances. Proc. Camb. Phil. Soc. **13**, 49-54.

Thum F. (1979). Sekundärelektronenemission durch Ionenbeschuß von Goldoberflächen. Thesis Techn. Univers. München, 1979; also Report IPP 9/29, Garching, Germany.

Thum F, Hofer WO. (1979). No Enhanced Electron Emission from High-Density Atomic Collision Cascades in Metals. Surface Sci. **90**, 331-338.

Thum F, Hofer WO. (1980). Ion-Induced Secondary Electron Emission by Heterogeneous Cluster Ions. SASP '80, Ed. E. Lindinger et al., Univ. Innsbruck, Austria. p. 19-21.

Thum F, Hofer WO. (1984). Z_1-Oscillations in Ion-Induced Kinetic Electron Emission. Nucl. Instr. Meth. Phys. Res. B**2**, 531-535.

Tougaard S, Sigmund P. (1982) Influence of elastic and inelastic scattering on energy spectra of electrons emitted from solids. Phys. Rev. B**25**, 4452-4466.

Veje J. (1981). Emission of secondary electrons and photons from silver bombarded with Sb^+, Sb_2^+ and Sb_3^+. Radiat. Effect. **58**, 35-39.

Villard PM. (1899). Sur Les Rayons Cathodiques. J. de Physique Theorique et Appliquee Ser. 3, No. 8, 5-16.

Waters PM. (1958). Kinetic Ejection of Electrons from Tungsten by Cesium and Lithium Ions. Phys. Rev. **111**, 1053-1061.

Wehner G. (1966). Energieverteilung der von 2, 5, 10 und 15 keV He- und Ar-Ionen an Molybdän ausgelösten Elektronen. Z. Physik **193**, 439-442.

Weizel W, Beeck O. (1932). Ionisierung und Anregung durch Ionenstoß. Z. Physik **76**, 250-259.

Werner HW, de Grefte HAM. (1965). Measurement of small ion currents in a mass spectrometer with a scintillation detector. Transact. 3rd Int. Vac. Congr., Stuttgart, **2**/2, 493-496.

Whaley R, Thomas EW. (1984). Auger spectra induced by Ne^+ and Ar^+ impact on Mg, Al, and Si. J. Appl. Phys. **56**, 1505-1513.

Wien K. (1989). Fast heavy ion induced desorption. Radiat. Eff. Def. Solids. **109**, 137-167.

Winter H. (1986). Sekundärelektronenemission bei Oberflächengitterführung leichter Ionen an Ni. Thesis Universität München.

Wittmaack K. (1979). Characteristics of ion-induced silicon L-shell Auger spectra. Surface Sci. **85**, 69-76.

Wolff PA. (1954). Theory of Secondary Electron Cascade in Metals. Phys. Rev. **95**, 56-66.

Zalm PC, Beckers LJ. (1984). Secondary Electron Yields from Clean Polycrystalline Metal Surfaces Bombarded by 5-20 keV Hydrogen or Noble Gas Ions. Philips J. Res. **39**, 61-76.

Zalm PC, Beckers LJ. (1985). Ion-Induced Secondary Electron Emission from Copper and Zinc. Surf. Sci. **152/153**, 135-141.

Zehner DM, Overbury SH, Havener CC, Heiland W. (1986). Electron emission from the interaction of multiply charged ions with a Au(110) surface. Surface Sci. **178**, 359-366; by the same group see also Phys. Rev. A **38**, 2294-2304.

Zscheile H. (1965). Zur Richtungsabhängigkeit der Sekundärelektronenausbeute von Kupfereinkristallen bei Ionenbeschuß. phys. stat. sol. **11**, 159-162.

Zwart ST de. (1987). Electron emission in collisions of Ar^{9+} on a tungsten surface. Nucl. Instr. Meth. Phys. Res. B**23**, 239-241.

Editor's Note: All of the reviewer's concerns were appropriately addressed by text changes, hence there is no Discussion with Reviewers.